REPORT DC-21 JANUARY, 1979

CSL COORDINATED SCIENCE LABORATORY

DECISION AND CONTROL LABORATORY

THE CONTROL OF MULTIVARIABLE SYSTEMS CONTAINING TIME DELAYS USING SMITH PREDICTORS

TENGKU AZZMAN SHARIFFADEEN IBRAHIM
D. GRANT FISHER

REPORT T-73

UNIVERSITY OF ILLINOIS - URBANA, ILLINOIS

THE CONTROL OF MULTIVARIABLE SYSTEMS CONTAINING TIME DELAY USING SMITH PREDICTORS

by

Tengku Azzman Shariffadeen Ibrahim
and
D. Grant Fisher

This work was supported in part by the National Science Foundation under Grant NSF INT-77-20969.

THE CONTROL OF MULTIVARIABLE SYSTEMS CONTAINING TIME DELAYS USING SMITH PREDICTORS

BY

Tengku Azzman Shariffadeen Ibrahim
Faculty of Engineering
University of Malaya
Kuala Lumpur 22-11
Malaysia
(On leave at Coordinated Science Laboratory,
University of Illinois at Urbana-Champaign)

and

D. Grant Fisher
Department of Chemical Engineering
University of Alberta
Edmonton, Alberta
Canada T6G 2G6

Urbana, Illinois

November 16, 1978

ABSTRACT

The Smith predictor method for the control of systems containing pure time delays is extended to multivariable systems with arbitrary delays in all control and output (or state) variables. Modified forms of predictor are suggested which can provide better performance and stability properties as compared to the conventional type. A design technique based on the Nyquist array is proposed which allows the incorporation of a Smith predictor into a multivariable system. System integrity to actuator or sensor failure is also analysed.

The above techniques of analysis and design are applied to a model of a two-input, two-output distillation column. Simulation results are presented comparing the various forms of predictor control with noninteracting control and independent single-loop PI control. These results indicate the advantages of modifying the conventional Smith predictor in the multivariable case. Good control can be obtained by employing the Smith predictor even for moderate time delays, especially for a set-point change. When the time delays are comparable to the plant time constants, the improvement in performance is greater.

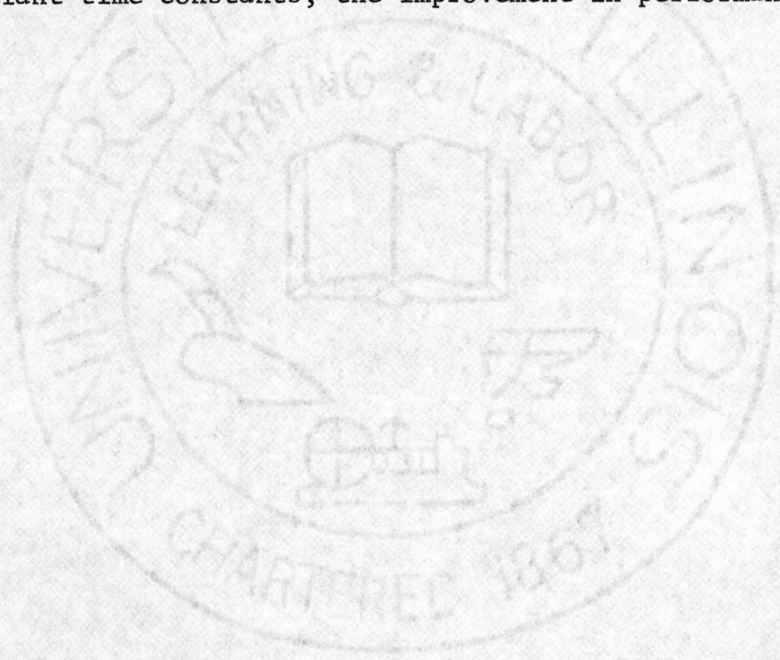

ACKNOWLEDGEMENT

The authors wish to thank Professor J. B. Cruz, Jr. for the use of the facilities at the Coordinated Science Laboratory in performing part of this work.

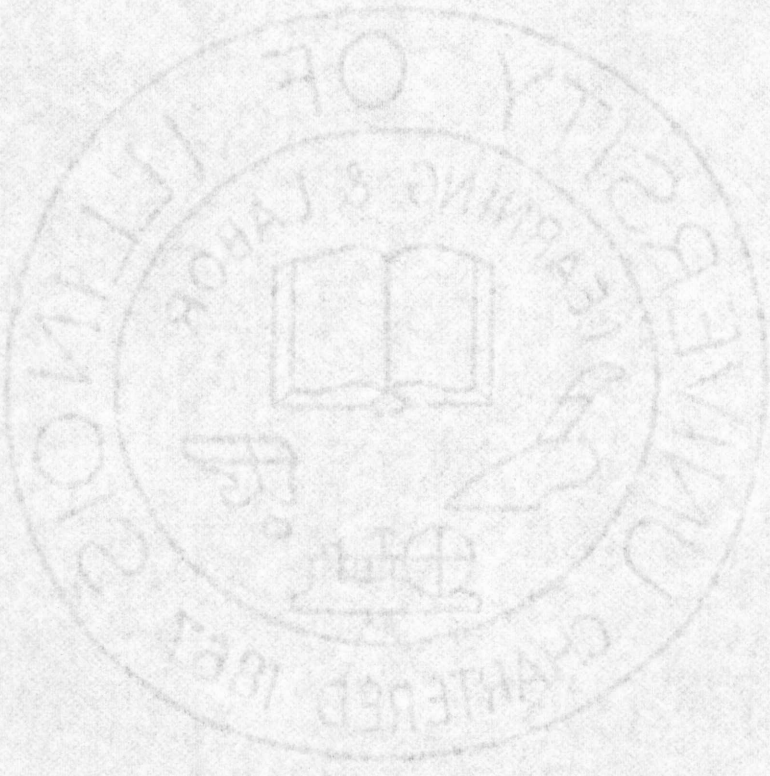

TABLE OF CONTENTS

CHAPTER		Page
1.	INTRODUCTION	1
2.	SMITH PREDICTORS FOR MULTIVARIABLE SYSTEMS	2
2.1.	The Conventional Smith Predictor	2
2.2.	Modified Smith Predictors	4
3.	DESIGN OF SYSTEMS INCORPORATING SMITH PREDICTORS	7
4.	INTEGRITY TO ACTUATOR OR SENSOR FAILURE	8
5.	CLOSED-LOOP FREQUENCY RESPONSE	11
6.	A DESIGN EXAMPLE: APPLICATION TO DISTILLATION COLUMN CONTROL	12
6.1.	The Plant	12
6.2.	Nyquist Array Design Incorporating Smith Predictors	13
6.3.	Noninteracting Control	17
6.4.	Independent Single-Loop PI Controllers	18
6.5.	Simulation Results	18
6.5.1.	System Simulation	18
6.5.2.	Disturbance in Feedflow	20
6.5.3.	Set-Point Change of 1% in Top and Bottom Composition	21
6.5.4.	A Hypothetical System	22
6.5.5.	Discussion of Simulation Results	25
6.6.	System Integrity to Actuator or Sensor Failure	27
6.7.	Predictor Implementation	29
7.	CONCLUSIONS	29
APPENDIX A:	SMITH PREDICTORS FOR MULTIVARIABLE SYSTEMS CONTAINING PURE TIME DELAYS	30
REFERENCES		33

1. INTRODUCTION

The control of systems containing time delays has received considerable attention in the literature due to the frequent occurrence of such systems, especially in the process industries. Time delays increase phase lag in systems, and, if they are significant, can cause greatly reduced stability margins and consequent difficulties in design. Thus, special methods have been proposed which attempt to alleviate the effect of time delays. Among them, the algorithms of Smith [1,2], Dahlin [3] and Moore, et al [4] are well-known.

Extensive studies [see for example 5 and 6] have been carried out on the Smith predictor pertaining to single-variable systems and the resulting characteristics of these systems have been analyzed. In the field of multivariable systems, Alevisakis and Seborg [7] extended the Smith predictor to two specific types of multivariable system: first, systems having the same time delay, T_o, in all output variables; and second, systems having the same time delay, T_i, in all control variables as well as the same time delay, T_o, in all output variables. Alevisakis [8] also derived a predictor for systems in which only some of the control variables are delayed. However, in order to derive this latter predictor, he imposed certain restrictions on the form of the precompensator matrix.

In this paper, a generalized Smith predictor for systems containing time delays of different magnitude in each control and each output (or state) variable is derived. A design technique based on the Nyquist array [9] is then proposed which enables the incorporation of the Smith predictor into a multivariable system. Furthermore, modified forms of the Smith predictor are suggested in order to obtain better performance of the resulting system as compared to the

conventional type of predictor. System integrity to actuator or sensor failure is also investigated.

The above techniques of analysis and design are applied to a model of a two-input, two-output distillation column. Simulation results are presented for the different types of Smith predictor described herein. These results are compared with designs based on noninteracting control and independent single-loop PI control. Finally, conclusions are drawn concerning the properties of multivariable systems incorporating Smith predictors.

2. SMITH PREDICTORS FOR MULTIVARIABLE SYSTEMS

2.1. THE CONVENTIONAL SMITH PREDICTOR

Consider the system shown in Figure 2.1, where $\underline{u}$ is an ℓ-vector and $\underline{y}$ is an m-vector; so that matrices $G(s)$, $K_1(s)$ and $K_2(s)$ are of dimensions $m \times \ell$, $\ell \times m$ and $m \times \ell$, respectively.

The plant $G(s)$ is assumed to contain time delays, $K_1(s)$ is an arbitrary nonsingular compensator and $K_2(s)$ is the Smith predictor. In Appendix A, it is shown that for a plant with transfer function matrix

$$G(s) = \begin{bmatrix} g_{11}(s)e^{-sT_{11}} & g_{12}(s)e^{-sT_{12}} & \cdots & g_{1\ell}(s)e^{-sT_{1\ell}} \\ \vdots & & & \vdots \\ g_{m1}(s)e^{-sT_{m1}} & g_{m2}(s)e^{-sT_{m2}} & \cdots & g_{m\ell}(s)e^{-sT_{m\ell}} \end{bmatrix} \tag{2.1}$$

the conventional Smith predictor is given by

$$K_2(s) = \begin{bmatrix} g_{11}(s)(1-e^{-sT_{11}}) & g_{12}(s)(1-e^{-sT_{12}}) & \cdots & g_{1\ell}(s)(1-e^{-sT_{1\ell}}) \\ \vdots & & & \vdots \\ g_{m1}(s)(1-e^{-sT_{m1}}) & g_{m2}(s)(1-e^{-sT_{m2}}) & \cdots & g_{m\ell}(s)(1-e^{-sT_{m\ell}}) \end{bmatrix} \tag{2.2}$$

The equivalent Smith predictor for a state-space model with arbitrary delays in the control and state variables are given by equations (A.10) and (A.11) in the appendix.

From (2.2), we observe that the Smith predictor is composed of two distinct models of the plant: one exactly like the plant and the other a model of the same plant but with all time delays removed. Physical insight into the action of the predictor is gained by manipulating the diagram in Figure 2.1 into the equivalent block diagram shown in Figure 2.2. We now distinguish the exact model of the plant which is denoted by D(s) from the delayless model M(s).

In the ensuing discussion, we assume for the sake of simplicity that the plant as a whole has a time delay of T seconds, so that G(s) may be written as

$$G(s) = G_o(s)e^{-sT} \tag{2.3}$$

It is easy to see that if the plant model D(s) is perfect, then $\underline{w}(s)$ is always zero. By feeding back $\underline{z}(s)$, the controller $K_1(s)$ generates control action to control the model M(s), and the plant is, in effect, in an open-loop condition. If we use as the delayless model M(s) the delayless part of the plant $G_o(s)$, it is easy to see that the model predicts the plant output T seconds in advance.

Figure 2.2 can be further simplified to the form shown in Figure 2.3, assuming the model D(s) is perfect. This diagram indicates clearly the action of the Smith predictor, that is, it eliminates all time delays from the closed-loop characteristic equation of the system.

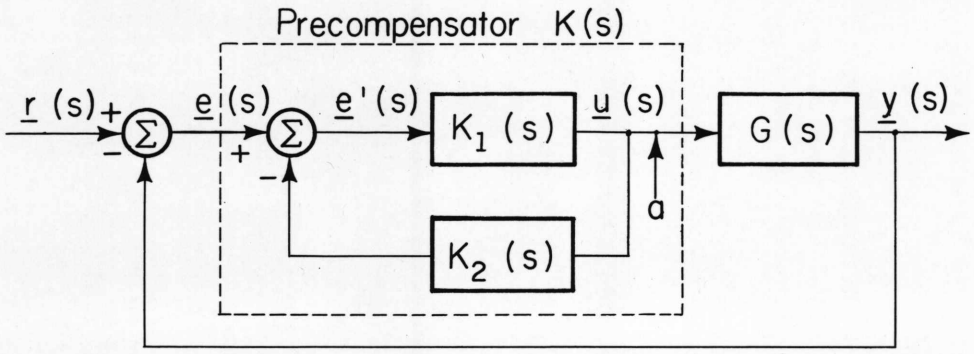

Fig. 2.1. Multivariable control system with inner-loop feedback.

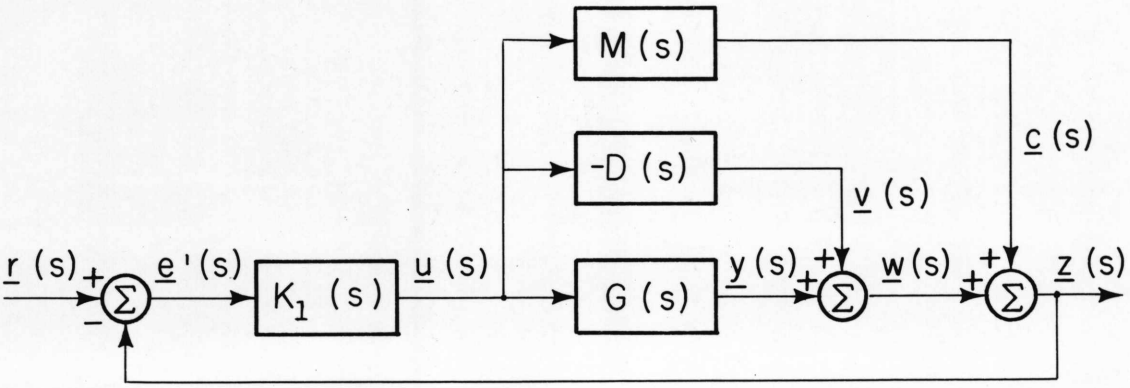

Fig. 2.2. Equivalent block diagram of Fig. 2.1 where $K_2(s)$ is replaced by Smith predictor $K_2(s) = M(s)-D(s)$.

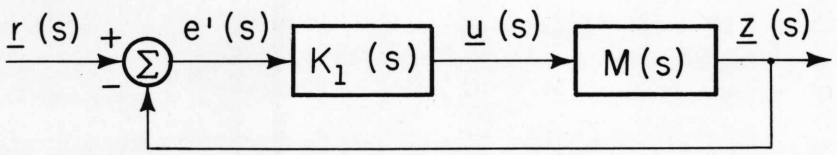

FP-6342

Fig. 2.3. Simplified block diagram of Fig. 2.2 for $D(s) = G(s)$.

Note that as long as the model D(s) duplicates the plant behavior exactly, we may in theory substitute any matrix for the delayless model M(s). However, we should bear in mind that the objective of a design is to control the plant. Thus, it would be more advantageous to generate control action that satisfies as closely as possible the requirements of the actual plant. In this particular case, $G_o(s)$ is the logical choice for the model M(s).

2.2 MODIFIED SMITH PREDICTORS

In the single-variable case, the Smith predictor is derived from the plant transfer function in a straightforward manner. Similarly, considering a multivariable plant with equal delays in all elements in the last section, we have found that derivation of the predictor is direct. In contrast, for multivariable systems containing arbitrary time delays which are, in general, different in all elements of G(s), we have added flexibility in the choice of the model M(s) to predict the behavior of the plant. In this section, we propose modified forms of the conventional predictor which can have improved stability and performance characteristics.

Consider the two-input, two-output plant in Figure 2.4a and the delayless model in Figure 2.4b. Figure 2.4b represents the delayless model M(s) considered in section 2.1. For the general case discussed here, this model may not be satisfactory for the following reason. By removing all time delays, the model output $\underline{c}(t)$ no longer predicts the actual plant output $\underline{y}(t)$. This is easily seen from the equations for the model outputs for any time t:

$$\left.\begin{aligned} c_1(t) &= \bar{c}_{11}(t) + \bar{c}_{12}(t) \\ &= \bar{y}_{11}(t+T_{11}) + \bar{y}_{12}(t+T_{12}) \\ \text{and } c_2(t) &= \bar{y}_{21}(t+T_{21}) + \bar{y}_{22}(t+T_{22}) \end{aligned}\right\} \qquad (2.4)$$

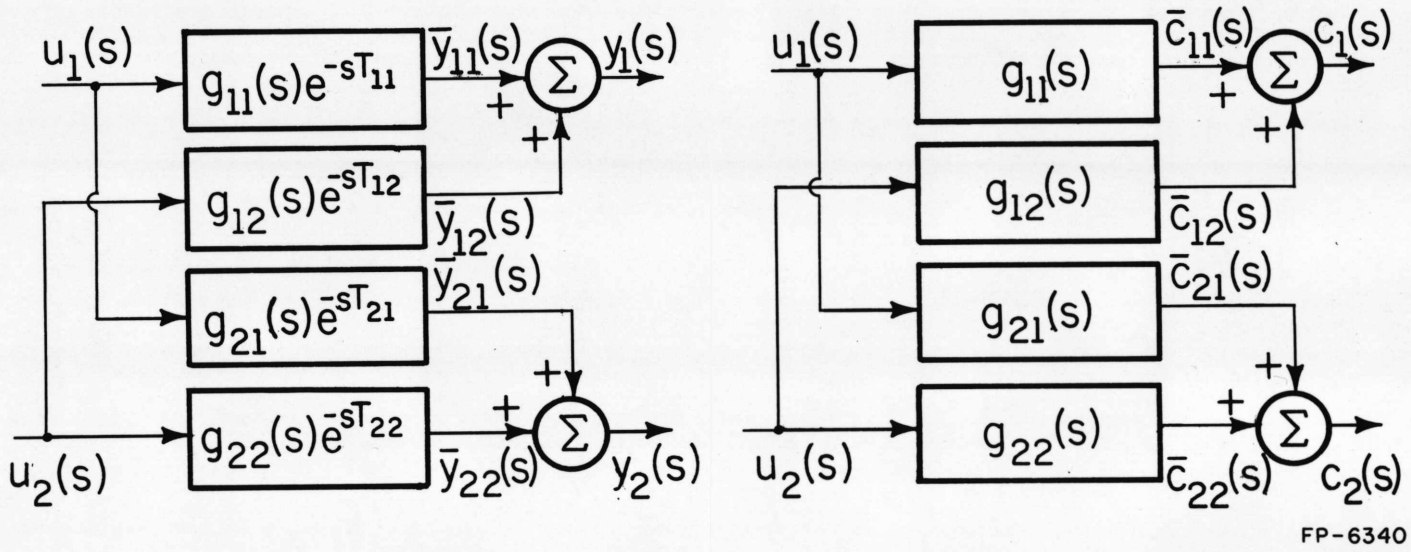

(a) Plant

(b) Delayless model

Fig. 2.4. Two-input, two-output process.

Equation (2.4) has no direct relationship to the actual plant outputs. For the special case where all delays are equal to T, which is considered in section 2.1, (2.4) reduce to

$$\left.\begin{aligned} c_1(t) &= y_1(t+T) \\ \text{and} \quad c_2(t) &= y_2(t+T) \end{aligned}\right\} \tag{2.5}$$

In this particular case, the model in Figure 2.4b is appropriate as it preserves the input-output behavior of the plant.

The above discussion suggests that, for the general case, a better choice for M(s) might be a model representing the plant with equal delays removed from all elements of its transfer function matrix. For example, if T_{11} is the smallest time delay in the plant of Figure 2.4a, the following model in (2.6) satisfies this requirement.

$$M(s) = \begin{bmatrix} g_{11}(s) & g_{12}(s)e^{-s(T_{12}-T_{11})} \\ g_{21}(s)e^{-s(T_{21}-T_{11})} & g_{22}(s)e^{-s(T_{22}-T_{11})} \end{bmatrix} \tag{2.6}$$

Delays greater than T_{11}, of course, can not be removed since the model M(s) would then be required to perform actual prediction of its own output.

The model in (2.6) would produce the following outputs.

$$\left.\begin{aligned} c_1(t) &= y_1(t+T_{11}) \\ c_2(t) &= y_2(t+T_{11}) \end{aligned}\right\} \tag{2.7}$$

which show that prediction of plant outputs by T_{11} seconds has been achieved.

It is noted in (2.6) that this model contains residual time delays which would tend to destabilize the system, and put to question the use of the predictor in the first place. An alternative approach is to remove as much time delay as possible from any row in the plant transfer function matrix, without requiring that all delays removed be the same for all rows. This can be verified to also correspond to a plant output predictor where the prediction time is different for different outputs. This is illustrated for the case $T_{11} < T_{12}$ and $T_{22} < T_{21}$ in (2.8).

$$M(s) = \begin{bmatrix} g_{11}(s) & g_{12}(s)e^{-s(T_{12}-T_{11})} \\ g_{21}(s)e^{-s(T_{21}-T_{22})} & g_{22}(s) \end{bmatrix} \tag{2.8}$$

An advantage of (2.8) or (2.6) might be that the residual delays now present are less detrimental to system stability and performance than before.

A third alternative is to employ a model which removes as much delay as possible from any column of the plant transfer function matrix, again without requiring the delays removed from all columns to be the same. Equation (2.9) illustrates the case where $T_{11} < T_{21}$ and $T_{22} < T_{12}$.

$$M(s) = \begin{bmatrix} g_{11}(s) & g_{12}(s)e^{-s(T_{12}-T_{22})} \\ g_{21}(s)e^{-s(T_{21}-T_{11})} & g_{22}(s) \end{bmatrix} \tag{2.9}$$

It can be shown that (2.9) corresponds to predicting plant inputs by T_{11} seconds and T_{22} seconds, respectively.

It is suggested that for the general case, the modified predictors incorporating either one of the models in (2.6), (2.8) and (2.9) may show better properties than the conventional type indicated in Figure 2.4b.

3. DESIGN OF SYSTEMS INCORPORATING SMITH PREDICTORS

In the form shown in Figure 2.1, it is difficult to design a compensator $K_1(s)$ for the plant $G(s)$. This is because $K_1(s)$ is within a minor loop formed with the predictor $K_2(s)$, so that no direct relationship exists between changes in $K_1(s)$ and the overall open-loop transfer function matrix $Q(s)$ given by

$$Q(s) = G(s)[I_\ell + K_1(s)K_2(s)]^{-1}K_1(s) \tag{3.1}$$

However, we have shown that Figure 2.1 can be manipulated into the form of Figure 2.3. We have now eliminated the minor loop and the design problem is considerably simplified. Note that we now design a controller for the model $M(s)$ instead of the plant $G(s)$. This is not a serious disadvantage for the the following reasons:

1) The model $M(s)$ is usually selected to behave as closely as possible to the plant, if not exactly so.
2) Although the signals $\underline{e}'(s)$ and $\underline{z}(s)$ are not the plant error and output signals, respectively, the control $\underline{u}(s)$ is the actual signal used to control the plant.
3) The asymptotic behavior as $s \to 0$ of $Q(s)$ given by (3.1) for any of the models discussed in section 2.2 is the same as that for $Q'(s)$ for the equivalent form in Figure 2.3, where

$$Q'(s) = M(s)K_1(s) \tag{3.2}$$

This implies that the steady-state error in $\underline{z}(t)$ is the same as that in $\underline{y}(t)$.

Utilizing the representation in Figure 2.3, any of the well-known design techniques can be employed to design the controller $K_1(s)$. In this paper, the Nyquist array method of Rosenbrock [9] is used. Rather than utilizing the inverse Nyquist array, we have chosen the direct Nyquist array for the reason that the model M(s) to be substituted for the real plant may also contain time delays in its elements. It is known that time delays cause inverse Nyquist diagrams to spiral outwards at high frequencies, thus making the achievement of diagonal dominance at these frequencies difficult. This difficulty is avoided by using direct Nyquist diagrams.

4. INTEGRITY TO ACTUATOR OR SENSOR FAILURE

System integrity to actuator or sensor failure is one of the important criteria in the selection of a control scheme. This property may also be employed to compare the different modifications to the Smith predictor discussed in section 2.2. Thus, in this section, we examine briefly the analysis of various failure conditions.

In a conventional Nyquist array design, system integrity to sensor failure can be deduced directly from the Nyquist array diagrams by inspection [9]. It turns out that for an open-loop stable plant, such a design is robust to changes in feedback gains from zero up to the maximum allowable gain in each loop. This property is lost in a system incorporating a predictor, thus requiring more detailed analysis.

Consider the block diagram shown in Figure 2.2, where we now assume for the sake of simplicity that the plant has two inputs and two outputs:

$$G(s) = \begin{bmatrix} g_{11}(s)e^{-sT_{11}} & g_{12}(s)e^{-sT_{12}} \\ g_{21}(s)e^{-sT_{21}} & g_{22}(s)e^{-sT_{22}} \end{bmatrix} \tag{4.1}$$

Let $D(s) = G(s)$ (a perfect model) (4.2)

and

$$M(s) = \begin{bmatrix} g_{11}(s)e^{-sT_{11}} & g_{12}(s)e^{-sT_{12}} \\ g_{21}(s)e^{-sT_{21}} & g_{22}(s)e^{-sT_{22}} \end{bmatrix} \tag{4.3}$$

Let there be an actuator failure in loop 1, such that the input to the plant is ku_1, where k is a constant and $0 \leq k < 1.0$.

The plant output vector is given by

$$\begin{bmatrix} y_1(s) \\ y_2(s) \end{bmatrix} = \begin{bmatrix} g_{11}(s)e^{-sT_{11}} & g_{12}(s)e^{-sT_{12}} \\ g_{21}(s)e^{-sT_{21}} & g_{22}(s)e^{-sT_{22}} \end{bmatrix} \begin{bmatrix} ku_1(s) \\ u_2(s) \end{bmatrix}$$

$$= \begin{bmatrix} kg_{11}(s)e^{-sT_{11}} & g_{12}(s)e^{-sT_{12}} \\ kg_{21}(s)e^{-sT_{21}} & g_{22}(s)e^{-sT_{22}} \end{bmatrix} \begin{bmatrix} u_1(s) \\ u_2(s) \end{bmatrix} \tag{4.4}$$

From Figure 2.2, we have

$$\underline{v}(s) = -D(s)\,\underline{u}(s) \tag{4.5}$$

and

$$\underline{w}(s) = \underline{v}(s) + \underline{y}(s) \tag{4.6}$$

Using (4.2), (4.4), (4.5) and (4.6), we get

$$\begin{bmatrix} w_1(s) \\ w_2(s) \end{bmatrix} = \begin{bmatrix} (k-1)g_{11}(s)e^{-sT_{11}} & 0 \\ (k-1)g_{21}(s)e^{-sT_{21}} & 0 \end{bmatrix} \begin{bmatrix} u_1(s) \\ u_2(s) \end{bmatrix} \tag{4.7}$$

We also have from Figure 2.2

$$\underline{z}(s) = \underline{w}(s) + \underline{c}(s) \tag{4.8}$$

Thus, using (4.3), (4.7) and (4.8) we obtain

$$\begin{bmatrix} z_1(s) \\ z_2(s) \end{bmatrix} = \begin{bmatrix} g_{11}(s)[(k-1)e^{-sT_{11}} + e^{-s\tau_{11}}] & g_{12}(s)e^{-s\tau_{12}} \\ g_{21}(s)[(k-1)e^{-sT_{21}} + e^{-s\tau_{21}}] & g_{22}(s)e^{-s\tau_{22}} \end{bmatrix} \begin{bmatrix} u_1(s) \\ u_2(s) \end{bmatrix} \tag{4.9}$$

or

$$\underline{z}(s) = G_{a1}(s)\underline{u}(s) \tag{4.10}$$

where $G_{a1}(s)$ is the transfer function matrix seen between $\underline{u}(s)$ and $\underline{z}(s)$ due to an actuator failure in loop 1.

It immediately follows that for a sensor failure in loop 1, the transfer function matrix $G_{s1}(s)$ seen between $\underline{u}(s)$ and $\underline{z}(s)$ is given by

$$G_{s2}(s) = \begin{bmatrix} g_{11}(s)[(k-1)e^{-sT_{11}} + e^{-s\tau_{11}}] & g_{12}(s)[(k-1)e^{-sT_{12}} + e^{-s\tau_{12}}] \\ g_{21}(s)e^{-s\tau_{21}} & g_{22}(s)e^{-s\tau_{22}} \end{bmatrix} \tag{4.11}$$

The result of failures in actuator 2 or sensor 2 can be analysed in a similar manner and the same analysis follows for systems of higher dimensions.

From Figure 2.2, we note that the return difference of the system due to failure in actuator 1 is given by

$$F(s) = I_2 + G_{a1}(s)K_1(s) \tag{4.12}$$

The stability of the system for this failure mode can be determined by plotting the frequency response of the determinant of the return difference in (4.12) and employing equation (A.3). Other failure modes may be investigated in the same way. Note that algebraic tests for stability such as the Routh array cannot be directly applied to polynomials containing transcendental terms. An added advantage of the frequency response approach is that it indicates the "closeness" of the system to instability, that is, its relative stability.

5. CLOSED-LOOP FREQUENCY RESPONSE

The manipulated block diagrams in Figure 2.2 and Figure 2.3 also allow the derivation of the closed-loop transfer functions of the system. Closed-loop behavior can be analysed by plotting the closed-loop frequency response and serves as another criterion for comparing different controllers.

For the system in Figure 2.2, we have

$$\underline{e}'(s) = [I_m + M(s)K_1(s)]^{-1}\underline{r}(s) \tag{5.1}$$

But from Figure 2.2, plant output y(s) is given by

$$\underline{y}(s) = G(s)K_1(s)\underline{e}'(s) \tag{5.2}$$

Using (5.1) and (5.2), we get

$$\underline{y}(s) = G(s)K_1(s)[I_m + M(s)K_1(s)]^{-1}\underline{r}(s) \tag{5.3}$$

or

$$\underline{y}(s) = H(s)\underline{r}(s) \tag{5.4}$$

where

$$H(s) = G(s)K_1(s)[I_m + M(s)K_1(s)]^{-1} \tag{5.5}$$

is the closed-loop transfer function matrix.

6. A DESIGN EXAMPLE: APPLICATION TO DISTILLATION COLUMN CONTROL

6.1. THE PLANT

The model to be utilized in this example is that of a 9 inch diameter 8 tray pilot scale distillation column at the Department of Chemical Engineering, University of Alberta. Previous studies of this column have been reported by Wood and Berry [10] and Wood and Pacey [11]. Details of the instrumentation and experimental derivation of the model can be found in Berry [12].

Simultaneous control of the overhead and bottom composition is attempted by employing reflux and steam flow as the manipulated variables. This results in a multivariable system with two inputs and two outputs as given below:

$$\begin{bmatrix} x_D(s) \\ x_B(s) \end{bmatrix} = \begin{bmatrix} \frac{12.8e^{-1s}}{16.7s+1} & \frac{-18.9e^{-3s}}{21.0s+1} \\ \frac{6.6e^{-7s}}{10.9s+1} & \frac{-19.4e^{-3s}}{14.4s+1} \end{bmatrix} \begin{bmatrix} R(s) \\ S(s) \end{bmatrix} + \begin{bmatrix} \frac{3.8e^{-8.1s}}{14.9s+1} \\ \frac{4.9e^{-3.4s}}{13.2s+1} \end{bmatrix} \xi(s) \tag{6.1}$$

where time is in minutes and the symbols are explained in Table 6.1 together

with their nominal values.

Table 6.1. Symbols used in model

Symbol	Meaning	Nominal Value
x_D	overhead product composition	96% wt. methanol
x_B	bottom product composition	0.5% wt. methanol
R	reflux flow rate	1.95 lb/min
S	steam flow rate	1.71 lb/min
ξ	change in feed flow rate about nominal operating condition	0.34 lb/min

The model was established by pulse testing and assuming that the dynamics are characterized by time delays and first-order lags.

6.2. NYQUIST ARRAY DESIGN INCORPORATING SMITH PREDICTORS

It is clear from the transfer function matrix given in (6.1) that a Smith predictor can be employed to advantage to reduce the effect of time delays on system stability and performance.

Denoting the plant transfer function matrix by G(s) as before, we see that the Smith predictor is given by

$$K_2(s) = M(s) - D(s) \tag{6.2}$$

where

$$D(s) = G(s) \tag{6.3}$$

and M(s) is a model of the plant to be chosen. For the conventional Smith

predictor, we choose the delayless model given in (6.4)

$$M_1(s) = \begin{bmatrix} \frac{12.8}{16.7s+1} & \frac{-18.9}{21.0s+1} \\ \frac{6.6}{10.9s+1} & \frac{-19.4}{14.4s+1} \end{bmatrix} \qquad (6.4)$$

The direct Nyquist array of (6.4) is given in Figure 6.1. It is evident that the array is not diagonal dominant. Dominance can be achieved with a simple constant compensator designed by column operations. Stability in loop 2 is first ensured by multiplying column 2 by -1 and then reducing the size of $g_{12}(jw)$ by adding to column 2 a multiple of column 1. Reduction of $g_{21}(jw)$ is also possible by adding to column 1 a multiple of column 2. The following column operations were performed:

i) Multiply column 2 by -1.

ii) Subtract from column 2,1.4 times column 1.

iii) Subtract from column 1,0.7 times column 2.

The above operations result in the Nyquist array shown in Figure 6.2 for the diagonal elements where the Gershgorin circles are drawn for row dominance. Clearly the system is stable for arbitrarily high gains in each loop. This observation, of course, cannot be extended directly to the actual process since the model accuracy at high frequencies is questionable.

The precompensator obtained by the above operations is given in (6.5).

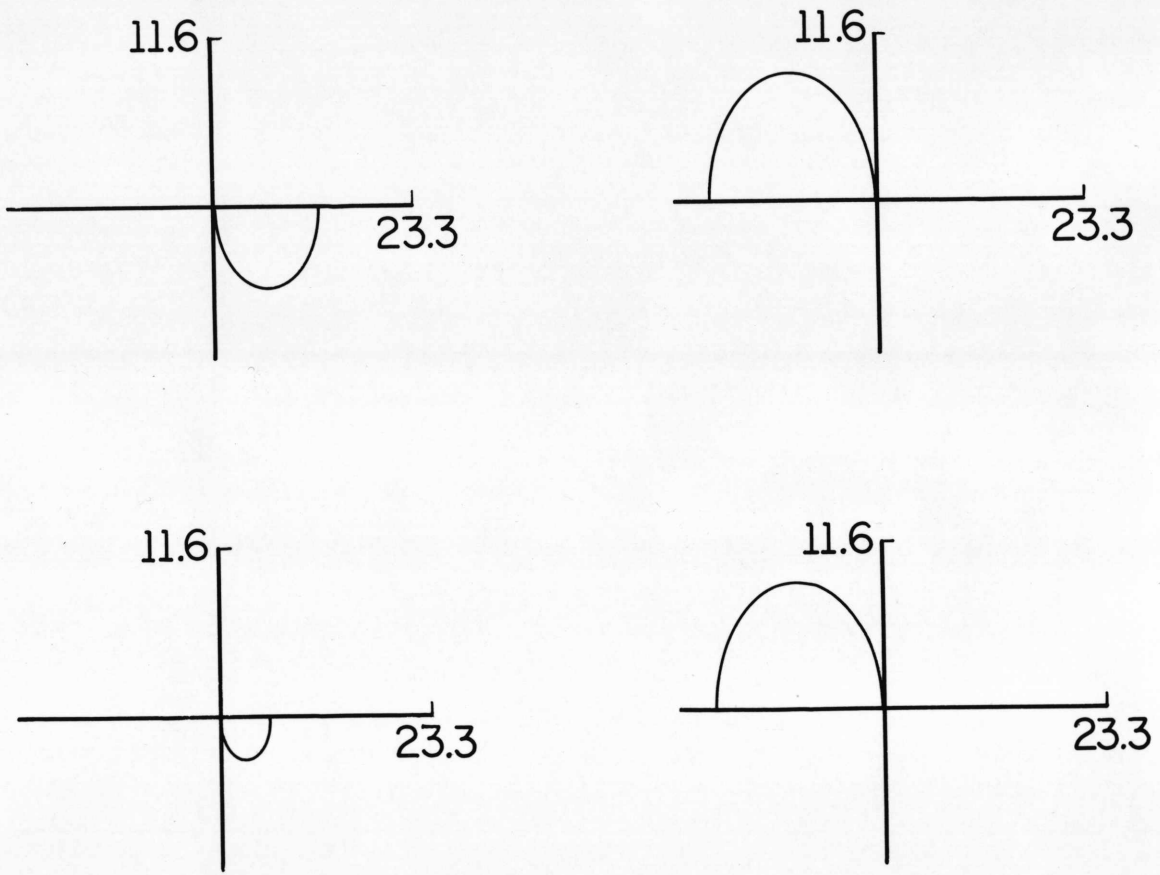

Fig. 6.1. Nyquist array of $M_1(s)$.

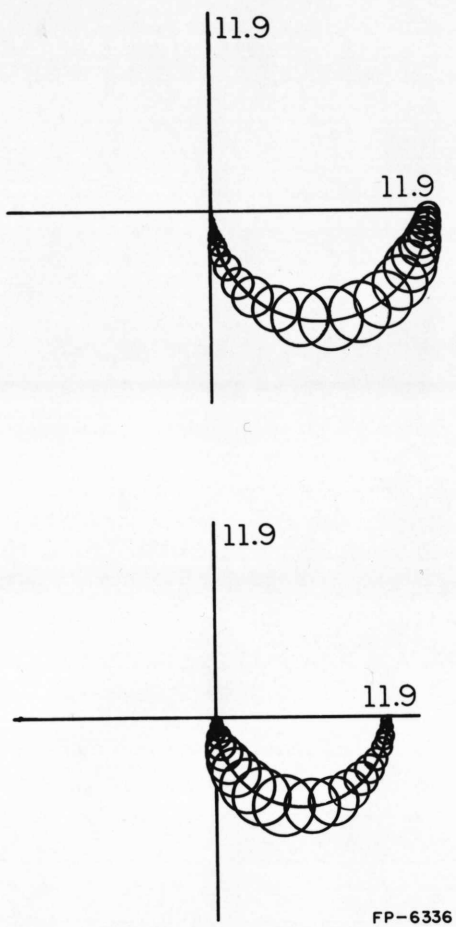

Fig. 6.2. Diagonal elements of compensated system with Gershgorin circles for row dominance.

$$K_1 = \begin{bmatrix} 1.98 & -1.4 \\ 0.7 & -1.0 \end{bmatrix} \tag{6.5}$$

From our discussion in section 2.2, several modifications can be made to the Smith predictor. One modification is to remove the largest time delay possible from all elements of the plant transfer function matrix, which results in the following model:

$$M_2(s) = \begin{bmatrix} \frac{12.8}{16.7s+1} & \frac{-18.9e^{-2s}}{21.0s+1} \\ \frac{6.6e^{-6s}}{10.9s+1} & \frac{-19.4e^{-2s}}{14.4s+1} \end{bmatrix} \tag{6.6}$$

Since the smallest time delay in the model is 1 min., its removal still leaves significant time delays in the three other elements of the matrix. In terms of control, we would expect that only low gains may be used in such a system. Consequently, this modification is not expected to yield good results.

A second modification can be effected by removing equal delays from any row, which also has an interesting physical interpretation as discussed in section 2.2. We would then have the model in (6.7).

$$M_3(s) = \begin{bmatrix} \frac{12.8}{16.7s+1} & \frac{-18.9e^{-2s}}{21.0s+1} \\ \frac{6.6e^{-4s}}{10.9s+1} & \frac{-19.4}{14.4s+1} \end{bmatrix} \tag{6.7}$$

Figure 6.3 shows the diagonal elements of the Nyquist array for $M_3(s)$ with Gershgovin circles for row dominance when the compensator in (6.5) is employed. Although the diagrams are less dominant compared to Figure 6.2, high gains can still be used in loop 1. For loop 2, permissible gain to ensure stability is now reduced (estimated to be about 0.6).

A third modification is to remove as much time delay in any column as possible. Carrying this out for the plant, we get the following model:

$$M_4(s) = \begin{bmatrix} \dfrac{12.8}{16.7s+1} & \dfrac{-18.9}{21.0s+1} \\ \dfrac{6.6e^{-6s}}{10.9s+1} & \dfrac{-19.4}{14.4s+1} \end{bmatrix} \tag{6.8}$$

By plotting the diagonal elements of $M_4(s)$ with Gershgorin circles for the compensator in (6.5), it is found as before that the dominance in element (2,2) has suffered, resulting in reduced allowable gains. Nevertheless, it did not appear essential to design a different compensator from (6.5) to improve loop 2. The use of the same compensator for the different types of predictor will also permit direct comparison of stability and performance characteristics.

Apart from the constant compensator in (6.5), integral action can be added to improve steady-state performance. The resulting PI controller will have the form

$$\bar{k}(s) = k_p + \frac{k_i}{s} \tag{6.9}$$

where k_p is the proportional constant and k_i is the integral constant.

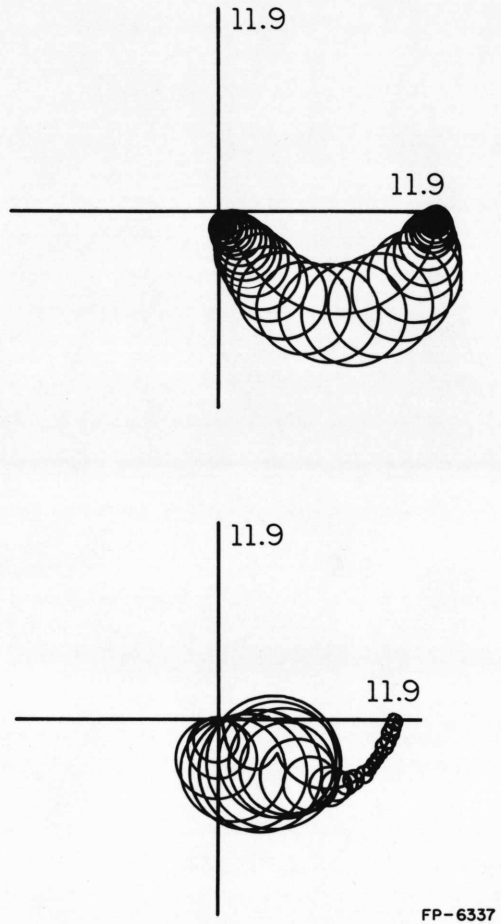

Fig. 6.3. Diagonal elements of compensated $M_3(s)$ with Gershgorin circles for row dominance.

6.3. NONINTERACTING CONTROL

The design of the noninteracting controller follows that of Zalkind [13,14]. The same type of controller is described in [10] and may be explained with reference to Figure 6.4 where we have suppressed the argument "s" for all variables.

The noninteracting controllers $k_{12}(s)$ and $k_{21}(s)$ are designed so that control action in one loop causes no interaction in the other loop. This is achieved by the following conditions:

$$\left.\begin{aligned} k_{21}(s)g_{22}(s) + g_{21}(s) &= 0 \\ \text{and} \qquad k_{12}(s)g_{11}(s) + g_{12}(s) &= 0 \end{aligned}\right\} \tag{6.10}$$

so that

$$\left.\begin{aligned} k_{21}(s) &= \frac{-g_{21}(s)}{g_{22}(s)} \\ \text{and} \qquad k_{22}(s) &= \frac{-g_{12}(s)}{g_{11}(s)} \end{aligned}\right\} \tag{6.11}$$

A check has to be made to ensure that (6.11) is realizable. In this particular case, by substituting for the elements of G(s) in (6.11) from (6.1), we have

$$\left.\begin{aligned} k_{21}(s) &= \frac{0.34(14.4s+1)e^{-4s}}{(10.9s+1)} \\ k_{12}(s) &= \frac{1.48(16.7s+1)e^{-2s}}{(21.0s+1)} \end{aligned}\right\} \tag{6.12}$$

which are clearly realizable.

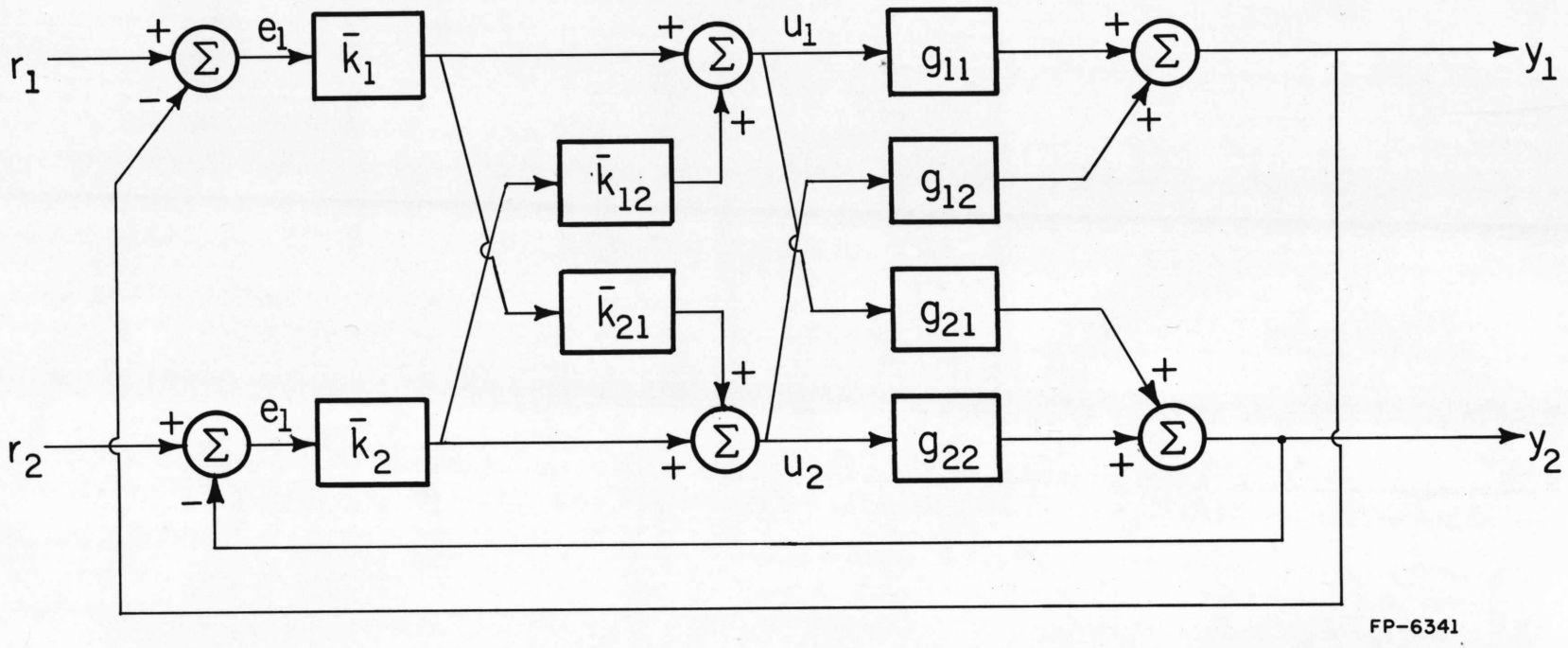

Fig. 6.4. Noninteracting control system.

PI controllers $\bar{k}_1(s)$ and $\bar{k}_2(s)$ may then be incorporated to improve steady-state error.

6.4. INDEPENDENT SINGLE-LOOP PI CONTROLLERS

This form of control is the easiest that may be attempted and is frequently used in industry. Two independent loops are closed around the plant and PI controllers tuned to obtain suitable response. The propositional and integral constants used in this study are those quoted in [10]. The results obtained would serve to compare the attainable performance for this type of control with the other types discussed.

6.5. SIMULATION RESULTS

6.5.1. SYSTEM SIMULATION

Extensive digital simulation was carried out using the IBM/360 CSMP program available at the University of Alberta. System response was obtained for two tests:

i) A disturbance in feed flow of +0.34 lb/min.

ii) Set-point change of +1% in each loop.

For purposes of comparison, the integral of the absolute error (IAE) was evaluated for each loop in a particular test. To ensure accuracy, IAE values at 400 min. were calculated.

Instead of using the compensator in (6.5) directly, the first column is normalized so that element (1,1) becomes unity, giving

$$K_2 = \begin{bmatrix} 1.0 & -1.4 \\ 0.35 & -1.0 \end{bmatrix} \qquad (6.13)$$

By this means, comparison of gain values between different designs becomes easier.

It has been noted in section 6.2 that the system incorporating the conventional Smith predictor would, in theory, be stable for arbitrarily high gains. At unrealistically high gains, the system can be arbitrarily fast with negligible steady-state error. Thus, in the simulation, it was found that although IAE values can be reduced at very high gains, the sensitivity of IAE to gain increase is reduced. Consequently, gains of 0.5 were arbitrarily selected for both loops which gave good response to a disturbance in feedflow. The effect of integral action also tended towards the same behavior, that is, at high integral constants the reduction in IAE to an increase in the constant is less. Therefore, integral constants were arbitrarily selected to obtain low IAE values. The same propotional and integral constants were used in all tests involving the various types of predictor and for both disturbance input and set-point change.

For the noninteracting system, the proportional and integral constants were obtained by tuning the loops to achieve the minimum IAE values to a disturbance in feedflow. Thus, the PI controllers in this case are the optimum for this plant. It will be noted that these constants are slightly different from those used in [10]. This is because the constants previously quoted were obtained by actual tuning on the plant, and also the actual process is computer-controlled, and is hence a sampled-data system which will exhibit slightly different characteristics from the continuous system.

No attempt was made to obtain optimum proportional and integral constants for the system controlled by independent single-loop PI controllers.

The same constants found to be optimum in [10] were used, and the resulting IAE values are again slightly different for the reasons given above.

6.5.2. DISTURBANCE IN FEEDFLOW

Of the four models discussed in section 6.2, only the models $M_1(s)$ (all delays removed) and $M_3(s)$ (equal delays removed from each row) exhibited good responses. Model $M_2(s)$ contained significant time delays to allow high gains to be used and model $M_4(s)$ did not perform as well as the model $M_3(s)$. Consequently, in this section, only results for predictors with $M_1(s)$ and $M_3(s)$ are presented.

Table 6.2 lists the proportional and integral constants utilized in the various tests together with the IAE values obtained.

Table 6.2. Proportional and integral constants and IAE values.

Type of controller	Loop 1			Loop 2		
	k_{p1}	k_{i1}	IAE	k_{p2}	k_{i2}	IAE
Smith predictor with $M_1(s)$	0.5	0.1	7.03	0.5	0.4	7.56
Smith predictor with $M_3(s)$	0.5	0.1	3.40	0.5	0.4	5.42
Noninteracting system	0.35	0.15	1.46	0.12	0.04	5.22
Independent PI control	0.2	0.045	4.98	0.04	0.015	12.97

Corresponding responses to a disturbance in feedflow are given in Figures 6.5, 6.6, 6.7 and 6.8, respectively. Comparison of the two types of Smith predictor reveals that the conventional predictor exhibits oscillaroty behavior, especially in the bottom composition. This is reflected in the IAE values which show the superiority of the modified predictor with $M_3(s)$. However,

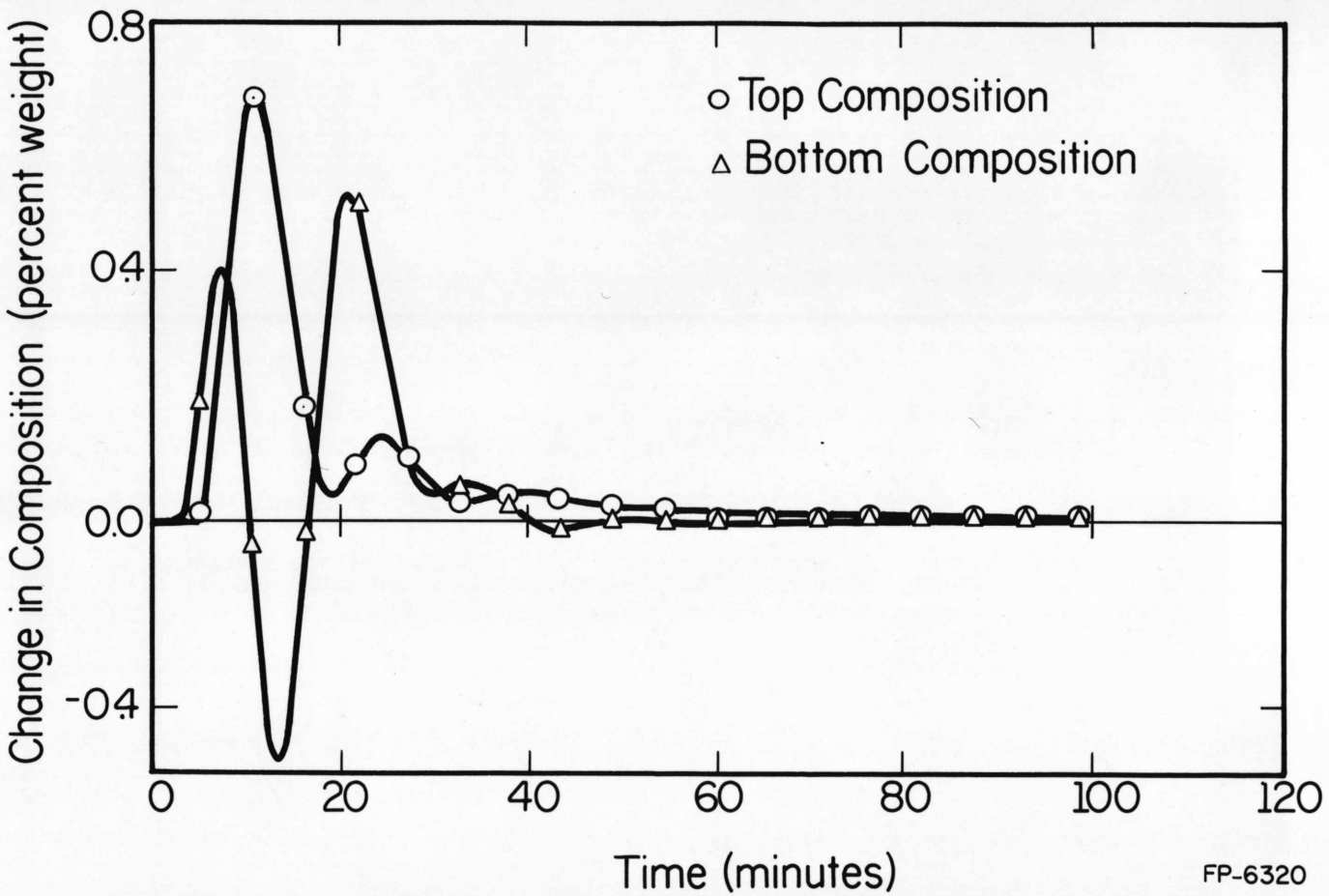

Fig. 6.5. Disturbance in feed flow - Smith predictor with $M_1(s)$.

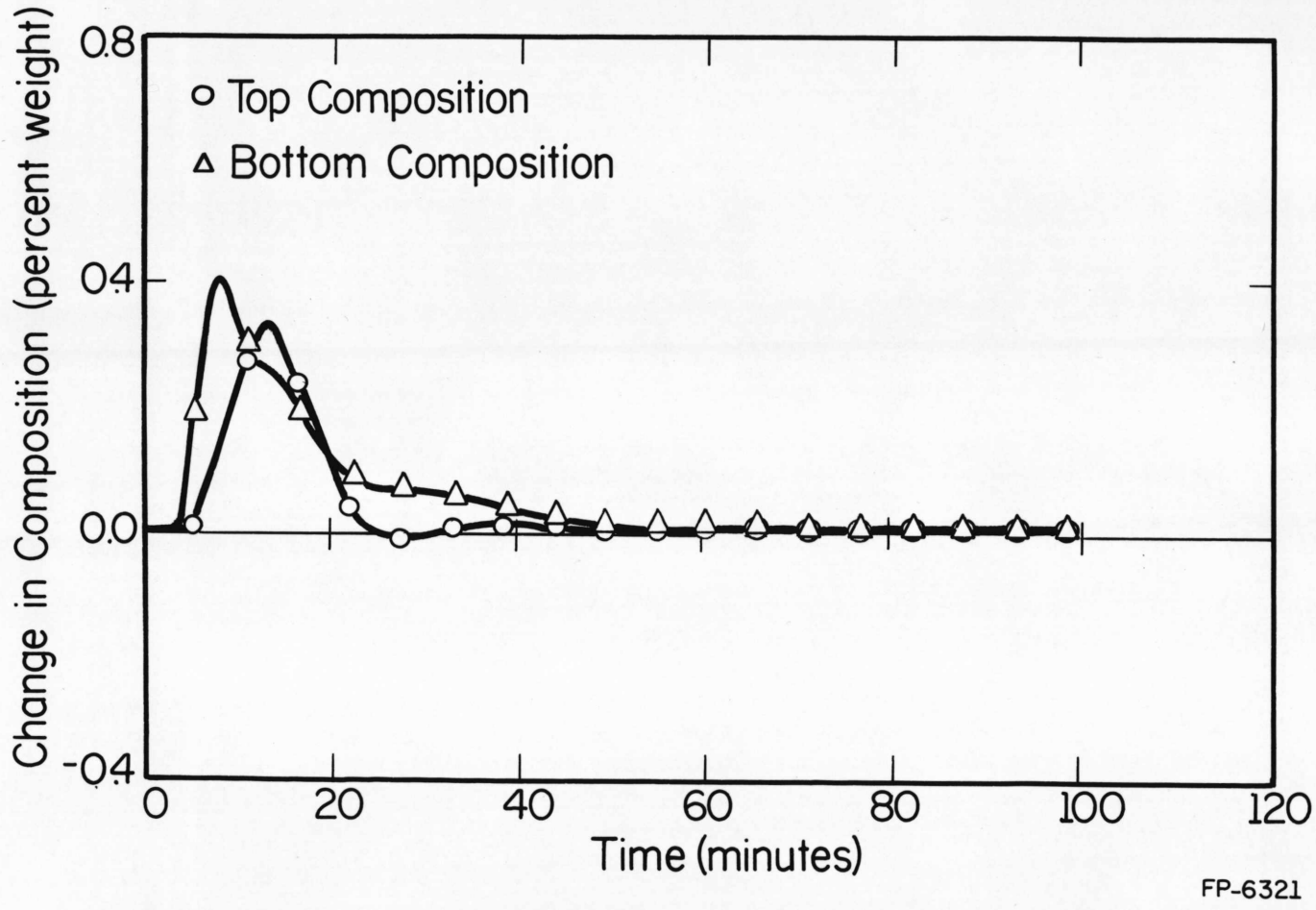

Fig. 6.6. Disturbance in feed flow - Smith predictor with $M_3(s)$.

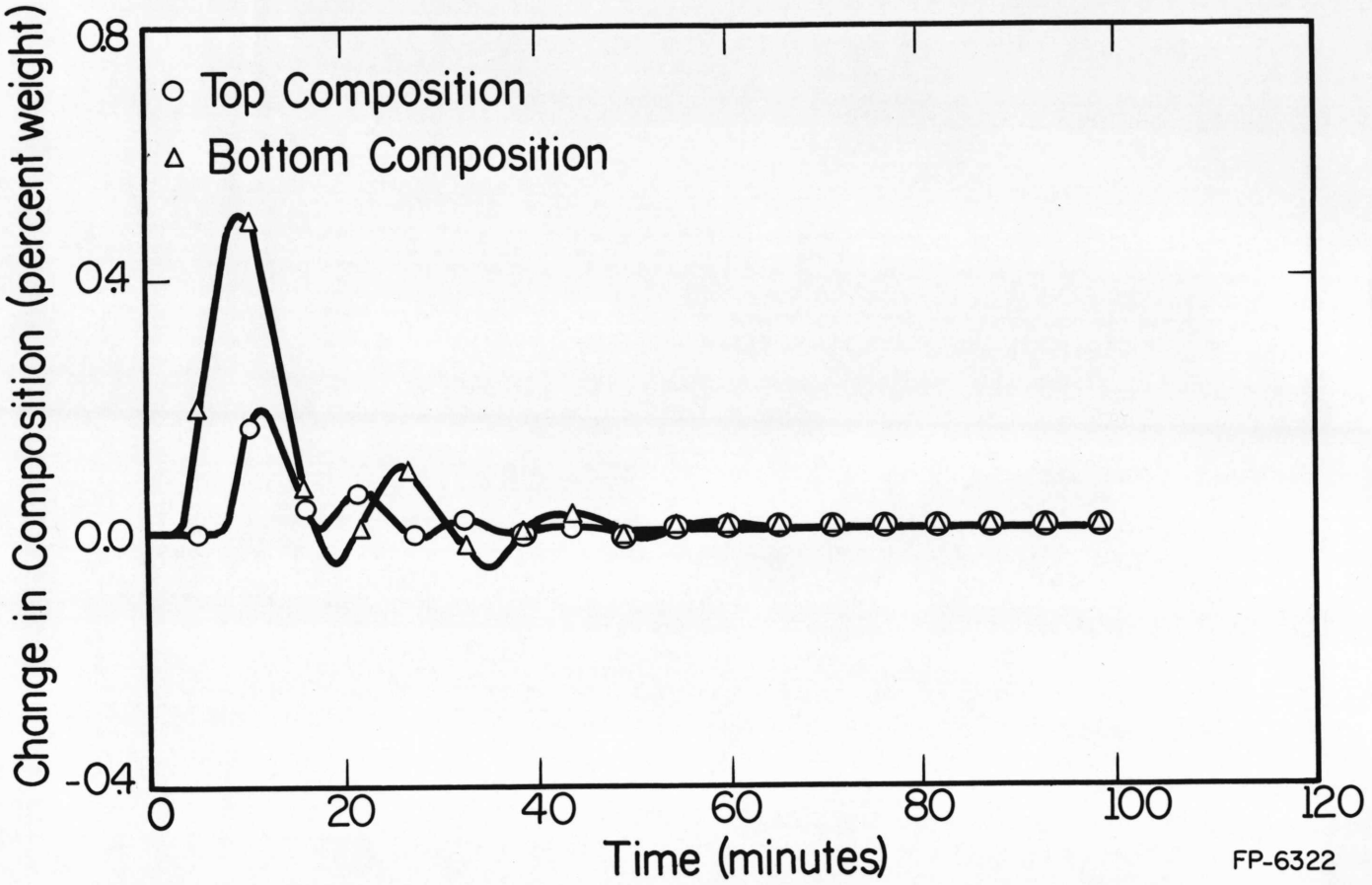

Fig. 6.7. Disturbance in feed flow - noninteracting system.

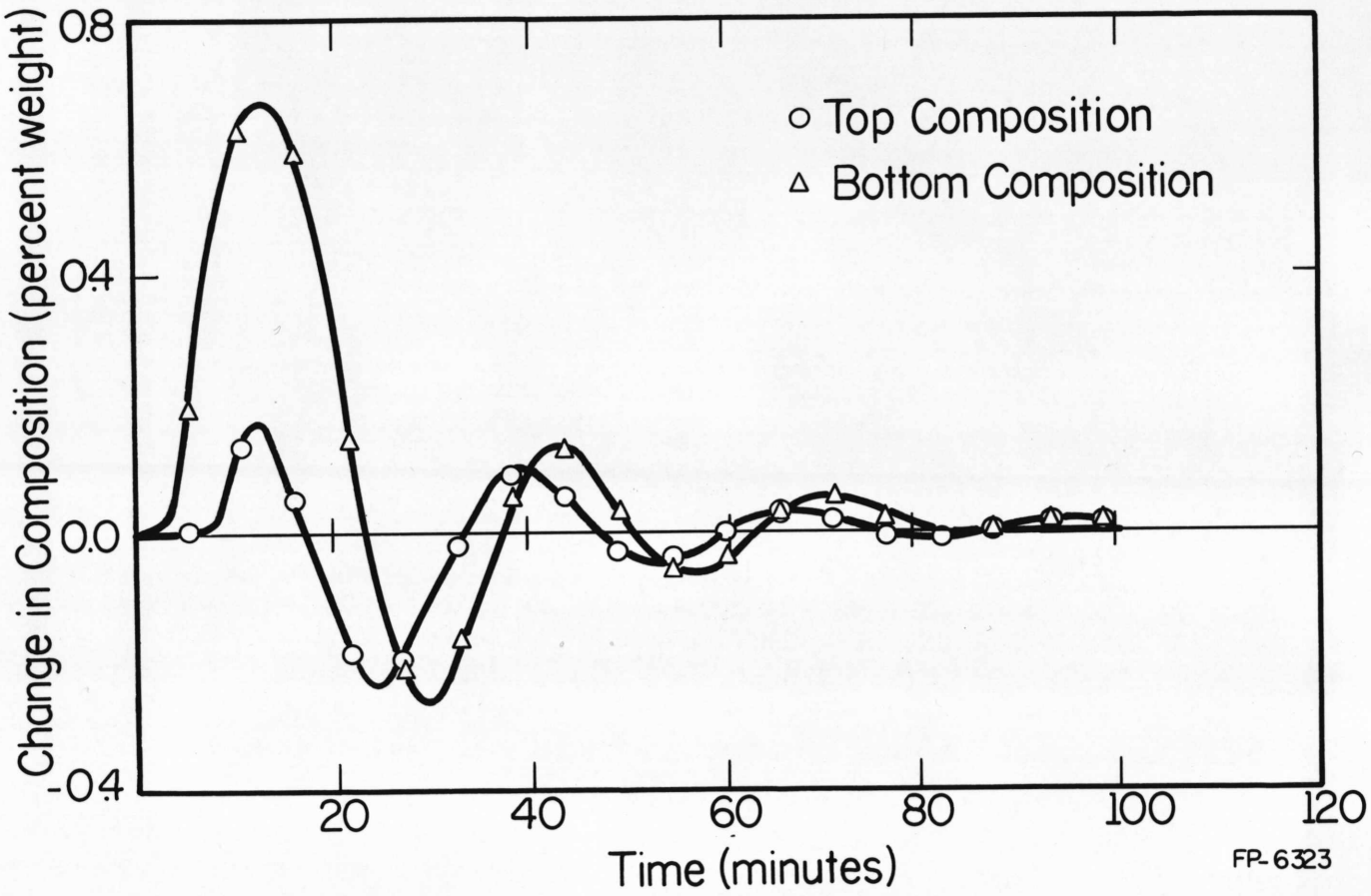

Fig. 6.8. Disturbance in feed flow - independent single-loop PI control.

the simulation indicates that noninteracting control results in even better control in the top composition. Bottom composition control is only marginally better than the modified predictor. Control by independent single-loop PI controllers for this process is generally not as good as the other types of control and demonstrates the advantage of reducing interaction.

6.5.3. SET-POINT CHANGE OF 1% IN TOP AND BOTTOM COMPOSITION

In this series of tests, the same PI controllers are used as given in Table 6.2. Table 6.3 presents the IAE values achieved.

Table 6.3. IAE values for set-point change.

Type of controller	Change in top composition		Change in bottom composition	
	IAE for Loop 1	IAE for Loop 2	IAE for Loop 1	IAE for Loop 2
Smith predictor with $M_1(s)$	4.19	8.26	9.48	17.05
Smith predictor with $M_3(s)$	5.83	1.34	2.87	4.65
Noninteracting system	6.29	-	-	11.89
Independent PI control	9.85	12.18	5.79	12.77

Figures 6.9-6.16 show the step responses of the system with the respective controllers. It is observed that although the noninteracting system offers better performance with regard to interaction, the modified predictor shows lower overall IAE values for the loop experiencing the set-point change. Again, the conventional predictor is highly oscillatory in both loops, resulting in large IAE figures. The low gains employed in the independent PI control

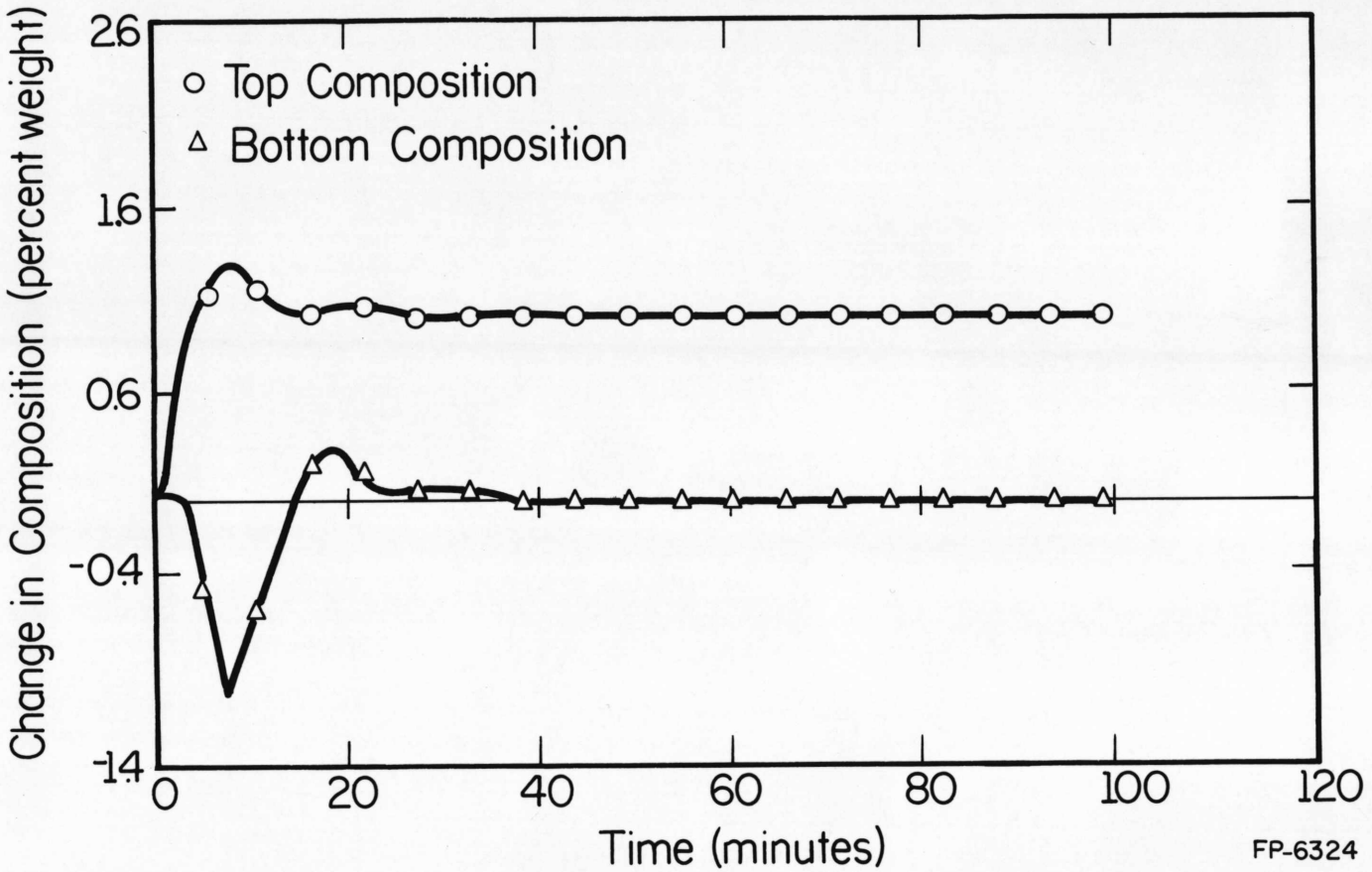

Fig. 6.9. Set point change in top composition - predictor with $M_1(s)$

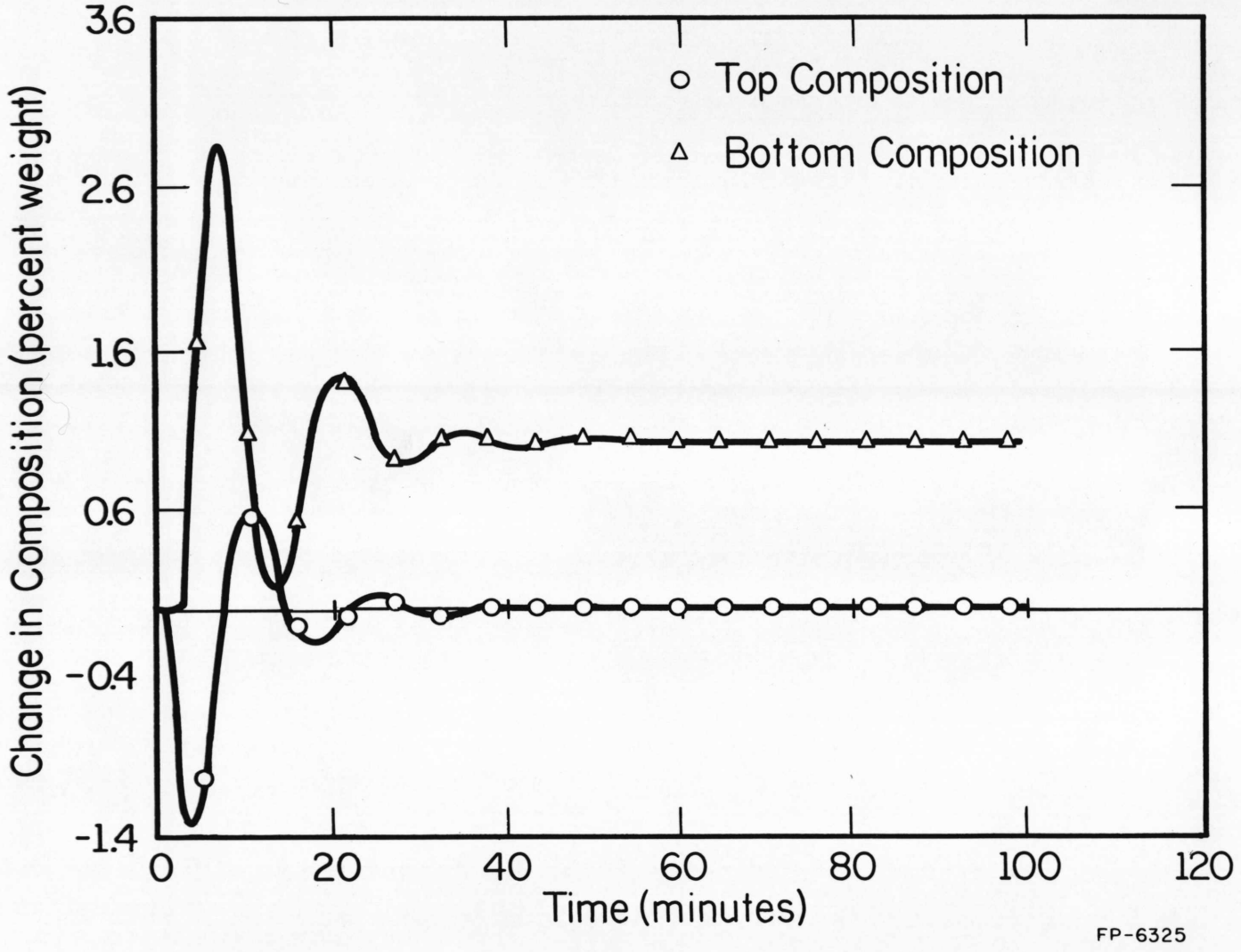

Fig. 6.10. Set point change in bottom composition - predictor with $M_1(s)$.

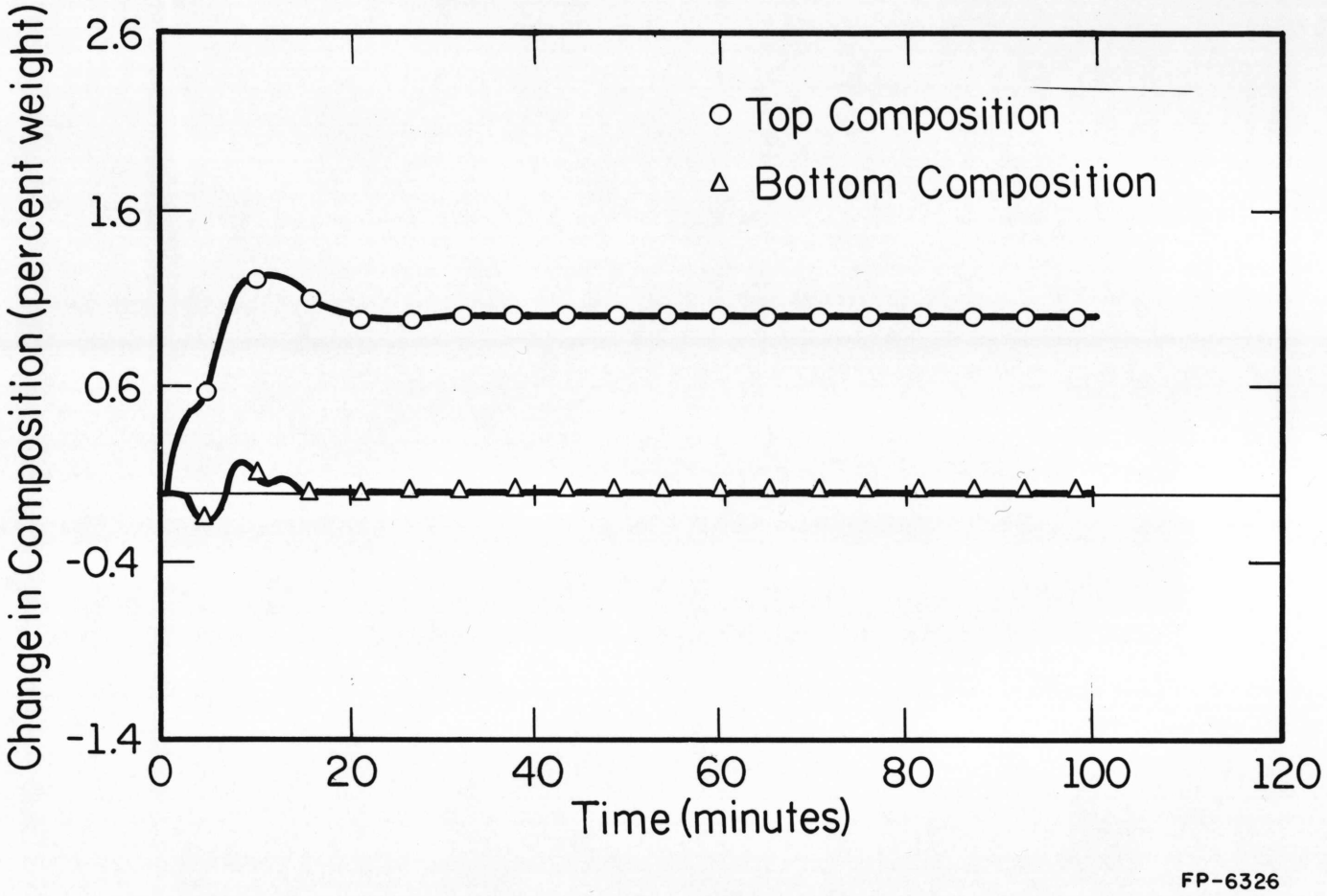

Fig. 6.11. Set point change in top composition - predictor with $M_3(s)$.

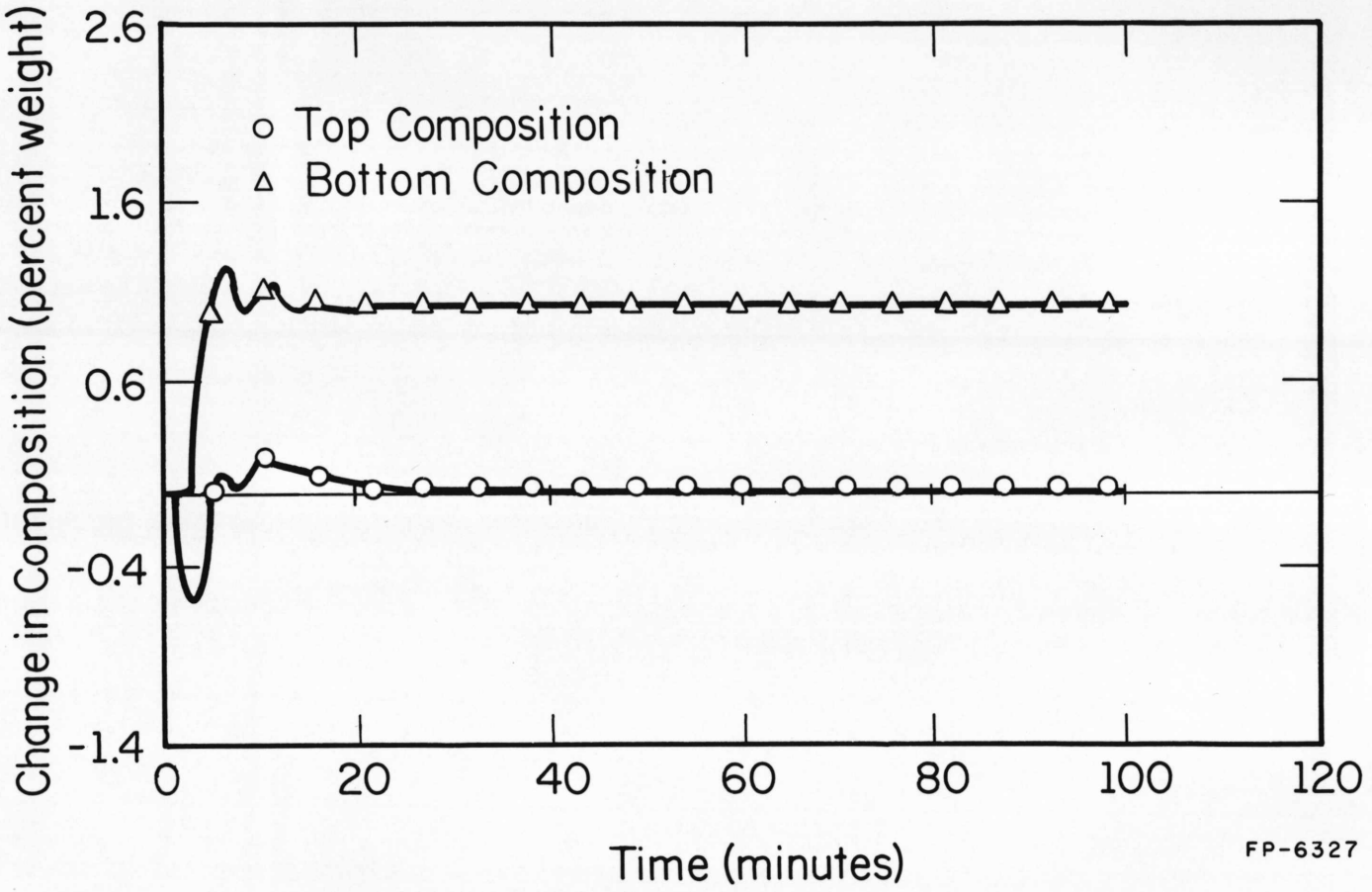

Fig. 6.12. Set point change in bottom composition - predictor with $M_3(s)$.

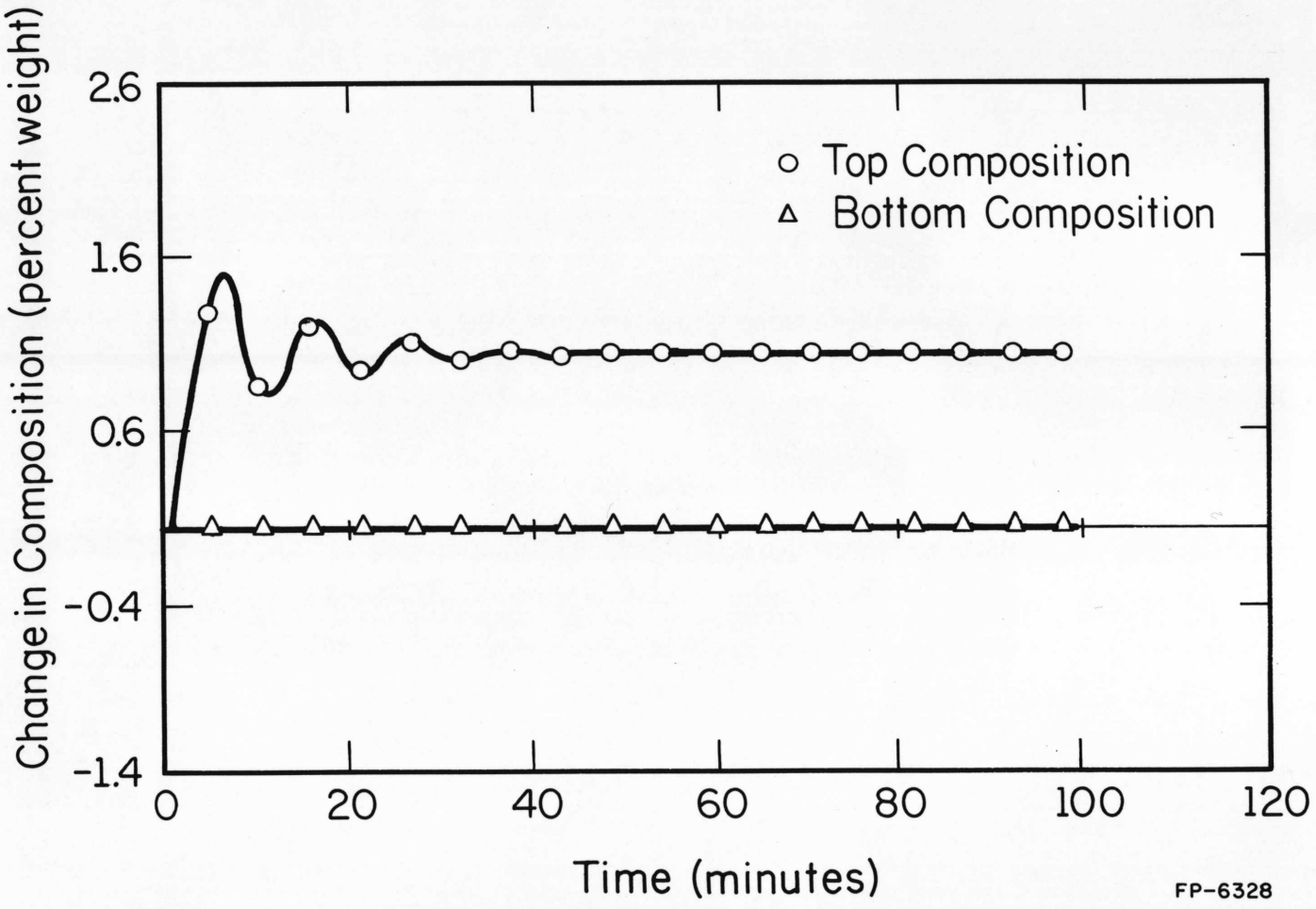

Fig. 6.13. Set point change in top composition - noninteracting system.

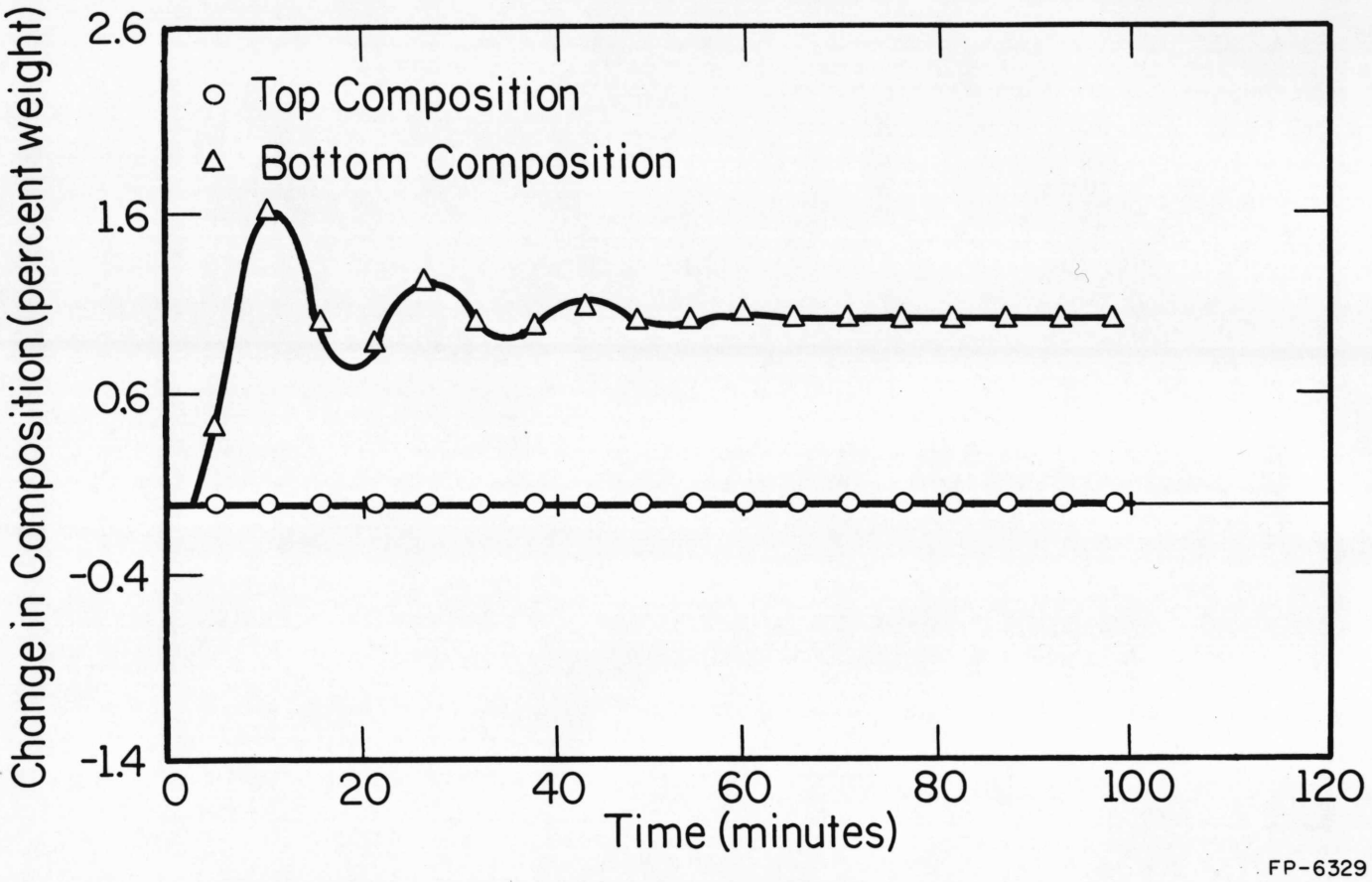

Fig. 6.14. Set point change in bottom composition - noninteracting system.

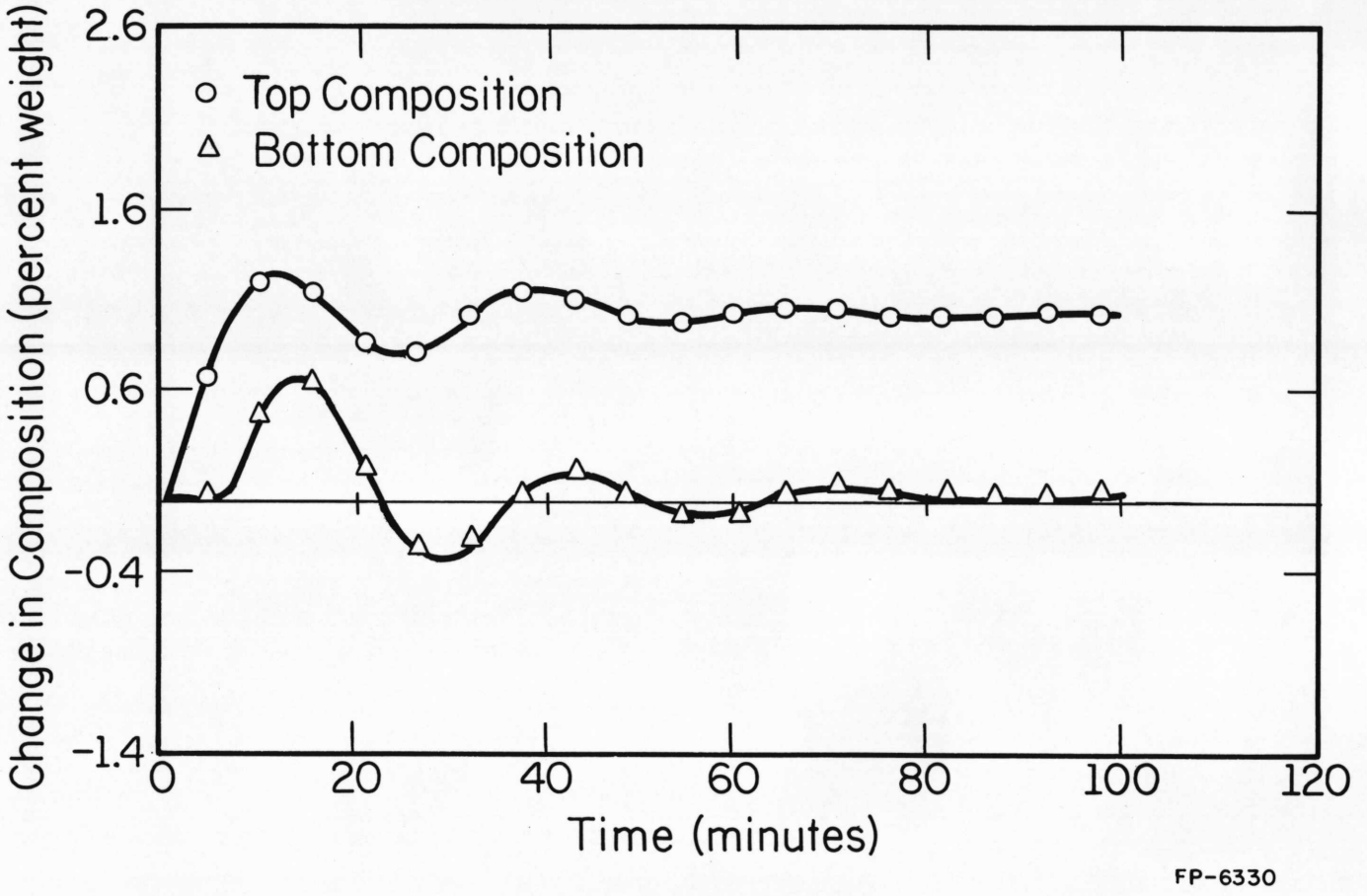

Fig. 6.15. Set point change in top composition - independent single-loop PI control.

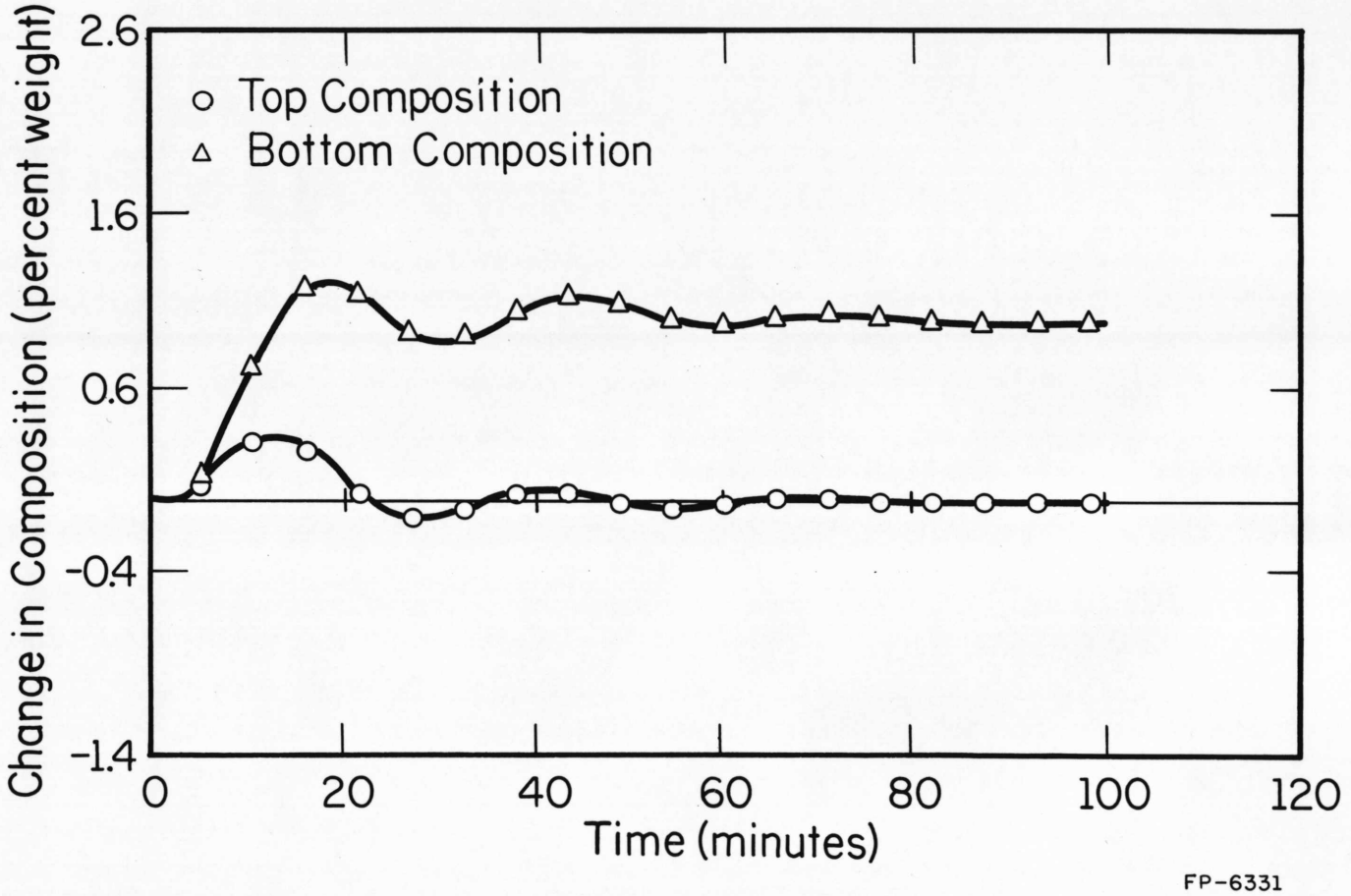

Fig. 6.16. Set point change in bottom composition - independent single-loop PI control.

scheme is reflected in the large IAE values obtained.

6.5.4. A HYPOTHETICAL SYSTEM

Previous studies of single-variable systems by Nielsen [5] concluded that for step inputs the improvement resulting from the use of the Smith predictor is greater when the pure time delay is small compared to the system time constants. Futhermore, it was found that for load (disturbance) changes the Smith predictor is of little value compared to conventional PI and PID controllers. Thus, it was decided to investigate the effect of increasing the time delays in the plant model, after observing the relatively small delays present as compared to the plant time constants.

The hypothetical plant in (6.13) is obtained by making the time delay in each row equal to the time constant of the diagonal element in the row concerned for the distillation column model in (6.1).

$$G(s) = \begin{bmatrix} \dfrac{12.8e^{-16.7s}}{16.7s+1} & \dfrac{-18.9e^{-16.7s}}{21.0s+1} \\ \dfrac{6.6e^{-14.4s}}{10.9s+1} & \dfrac{-19.4e^{-14.4s}}{14.4s+1} \end{bmatrix} \qquad (6.13)$$

Physically, this corresponds to a process with pure time delays of 16.7 min. and 14.4 min, respectively, at the outputs which may be due to measuring equipment placed at these points.

The form of the transfer function matrix suggests the model $M_1(s)$ given in (6.4) and the modified form $M_5(s)$ as below

$$M_5(s) = \begin{bmatrix} \dfrac{12.8e^{-2.3s}}{16.7s+1} & \dfrac{-18.9e^{-2.35s}}{21.0s+1} \\ \dfrac{6.6}{10.9s+1} & \dfrac{-19.4}{14.4s+1} \end{bmatrix} \tag{6.14}$$

which results from the removal of equal delays of 14.4 min. from all elements of the matrix.

Obviously the precompensator in (6.5) can again be utilized in this system. Proportional and integral constants were arbitrarily selected for the conventional predictor system to obtain low IAE values to a disturbance input. Use of the same constants for the model $M_5(s)$ resulted in highly oscillatory response in loop 1 due to the residual time delays. Consequently, the proportional and integral constants in this loop were reduced to give improved IAE figures, leaving the PI controller in loop 2 unchanged.

A noninteracting controller was designed based on the method described in section 6.3. PI controllers were then tuned to achieve the minimum IAE values to a disturbance input.

The proportional and integral constants employed are presented in Table 6.4, while Table 6.5 shows the IAE values obtained for a set-point change and disturbance input, where load transfer functions as in (6.1) are assumed.

Table 6.4. Proportional and integral constants.

Type of controller	Loop 1		Loop 2	
	k_{p1}	k_{i1}	k_{p2}	k_{i2}
Smith predictor with $M_1(s)$	1.4	0.12	1.4	0.1
Smith predictor with $M_5(s)$	1.0	0.06	1.4	0.1
Noninteracting system	0.17	0.0061	0.1	0.005

Table 6.5. IAE values to disturbance input and set-point change.

Type of controller	Disturbance input		Unit set-point change in loop 1		Unit set-point change in loop 2	
	IAE in Loop 1	IAE in Loop 2	IAE in Loop 1	IAE in Loop 2	IAE in Loop 1	IAE in Loop 2
Smith predictor with $M_1(s)$	23.1	25.7	18.2	0.6	0.9	15.8
Smith predictor with $M_5(s)$	21.7	25.7	22.9	1.3	2.5	16.0
Noninteracting system	35.5	39.1	36.9	-	-	31.3

This example emphasises clearly the high proportional and integral constants that can be employed when a Smith predictor is included in a system. Comparing with the noninteracting system, the IAE values achieved with a predictor for disturbance inputs is far superior. It is interesting to note that the predictor with $M_5(s)$ gives a lower IAE value in loop 1 although lower PI constants are employed. Figures 6.17, 6.18 and 6.19 show the responses to a disturbance input so as to facilitate visual comparison.

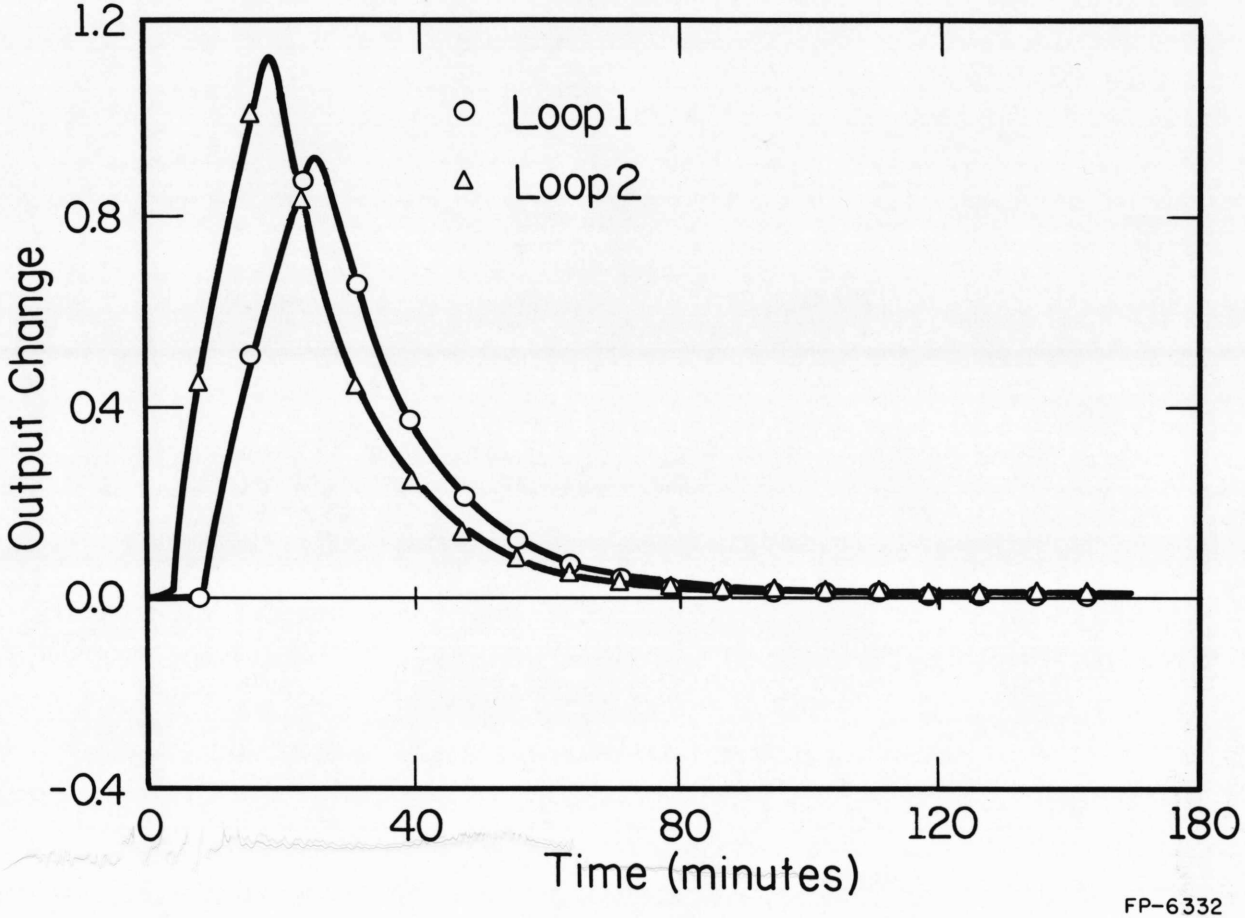

Fig. 6.17. Response to disturbance - predictor with $M_1(s)$.

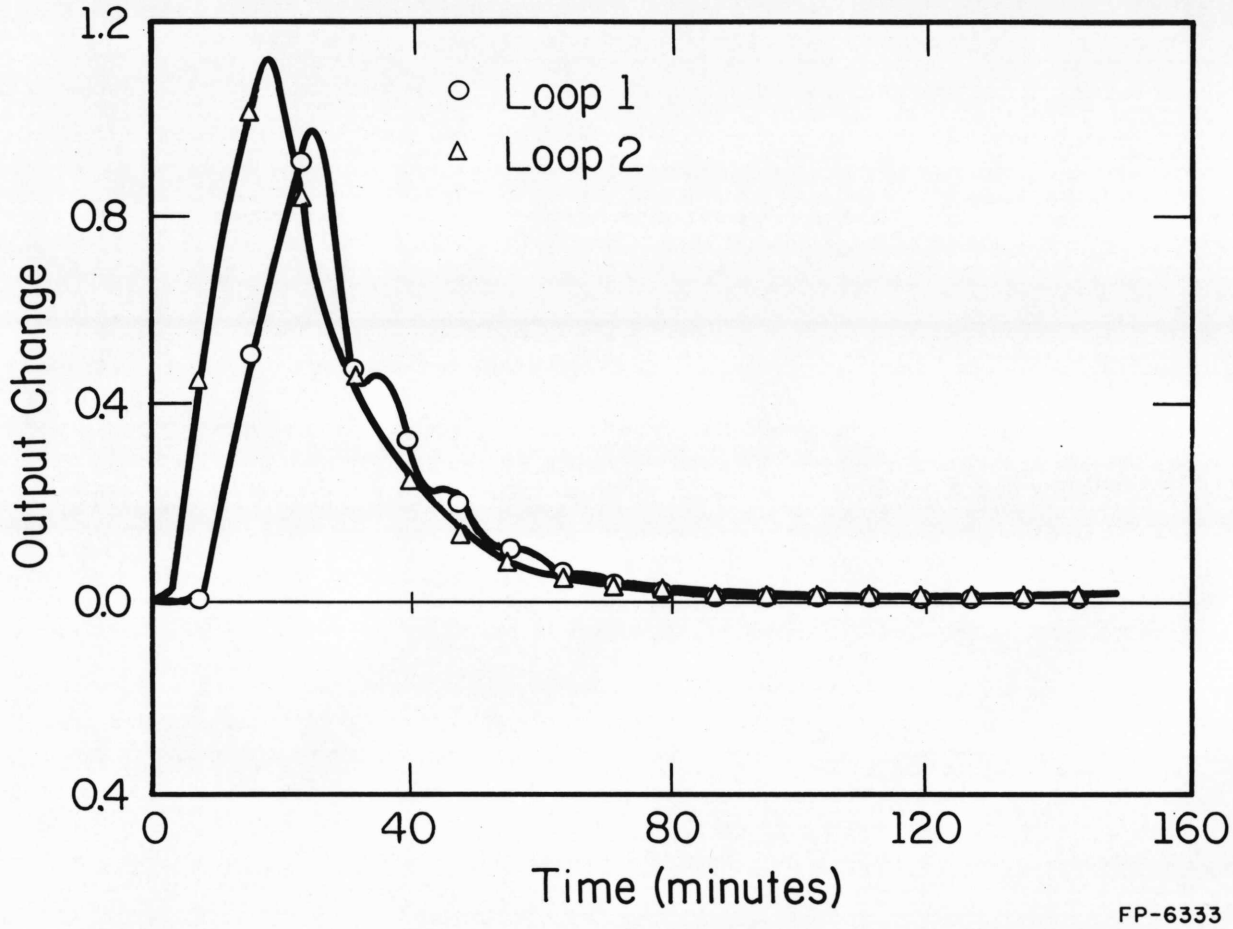

Fig. 6.18. Response to disturbance - predictor with $M_5(s)$.

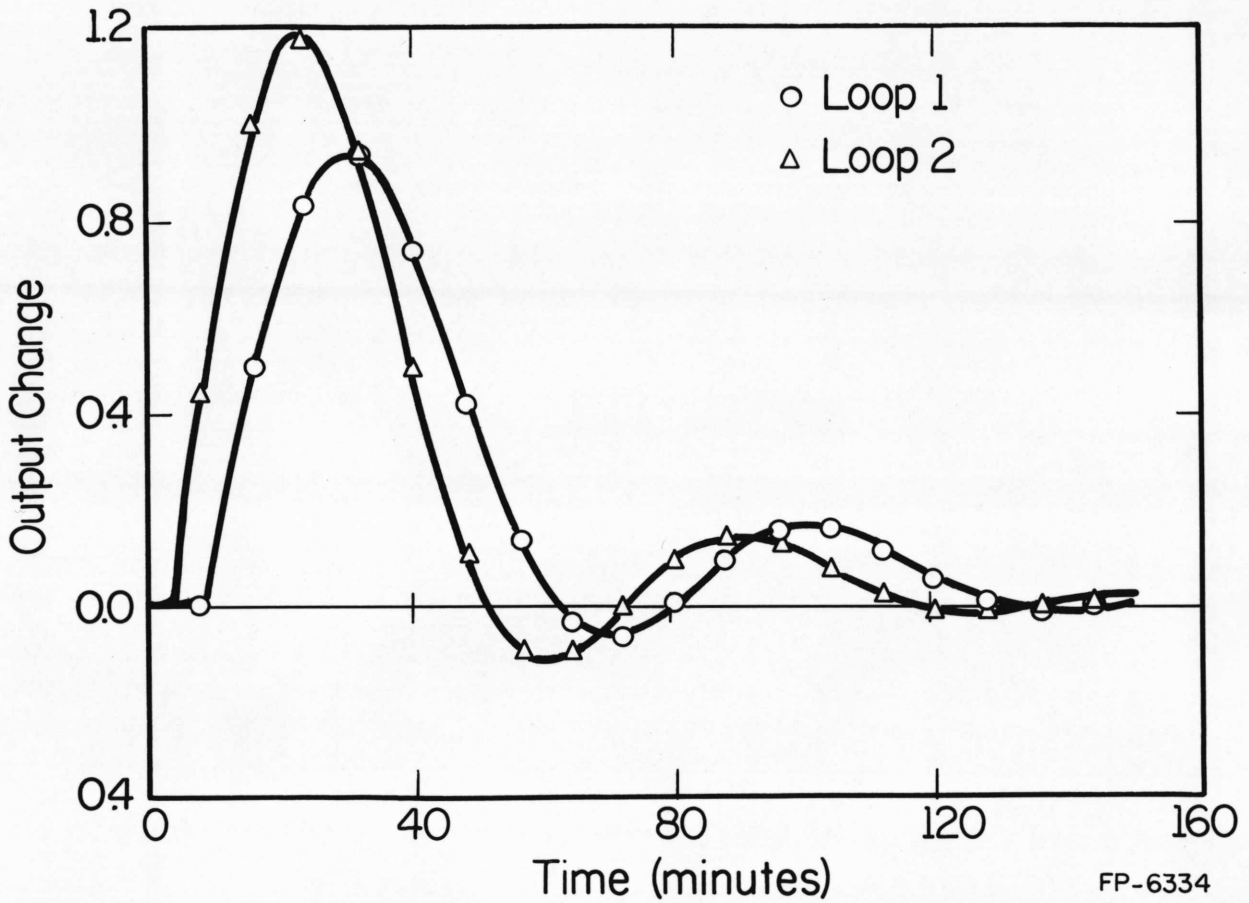

Fig. 6.19. Response to disturbance - noninteracting system.

The superiority of predictor control is even more marked for set-point changes, the IAE values attained with the conventional predictor being roughly half of those attained by the noninteracting controller. In this case, however, the predictor with $M_5(s)$ is not as good as the version with $M_1(s)$.

6.5.5. DISCUSSION OF SIMULATION RESULTS

The objective of carrying out the simulation was to compare the performance of the various types of predictors with other control schemes that are commonly implemented. However, comparison of performance is a difficult task, depending largely on the criteria employed. In this case, predictor control has been compared to noninteracting control and to independent single-loop PI control, using IAE values as a basis.

Comparison to noninteracting control serves two purposes. First, the previous study of this process by Wood and Berry [10] demonstrated that the noninteracting controller gave the best IAE values when compared to ratio control and control by independent single-loop PI controllers. Thus, by again employing the noninteracting controller as a standard, attainable IAE values for other controllers can be meaningfully compared. Secondly, the noninteracting controller is a special case of the Nyquist array design. It is expected that a design based on the Nyquist array using a simpler decoupling matrix would exhibit similar behavior. We have thus avoided the need to compare with another popular type of controller.

The use of IAE values as a performance index is purely arbitrary since any of the other measures of performance could have been used. However, the IAE criterion is a popular measure in industry and it also facilitates the direct connection with related work by Nielsen [5], Meyer et al [6] and Wood

and Berry [10] already quoted.

The first observation to make concerning predictor control is that it allows much higher gains and stronger integral action to be employed. As a result, the IAE values produced are correspondingly lower. It was previously noted that the removal of equal delays of 1 min. in all elements of the distillation column model is not satisfactory since the remaining delays would destabilize the system. Removing equal delays for any column also produced poor performance.

In order to see why this is so, we examine the closed-loop frequency response of the various predictor systems using equation (5.5). Figures 6.20, 6.21 and 6.22 show the closed-loop frequency response of the predictor schemes using model $M_1(s)$, $M_3(s)$ and $M_4(s)$, respectively. The compensator in (6.13) is used throughout, together with proportional gains of 0.5 in each loop. For purposes of comparison, we include Figure 6.23 which shows the closed-loop frequency response of the system in Figure 2.3 with $M(s) = M_1(s)$ (plant with all delays removed) and the compensator as defined above. It is observed that for all the predictor schemes, resonant frequencies are excited, the end result being oscillatory behavior and deterioration in IAE values. Comparison of the frequency responses for the three predictor schemes indicates that the predictor with $M_3(s)$ has the least resonant behavior, a fact already noted with regard to IAE performance.

These resonant modes are excited by the loss of a direct relationship between the predicted output and the actual plant output, as discussed in section 6.2. To preserve this relationship, equal delays from all elements have to be removed, a solution which is also unacceptable in this example due to the large residual delays present.

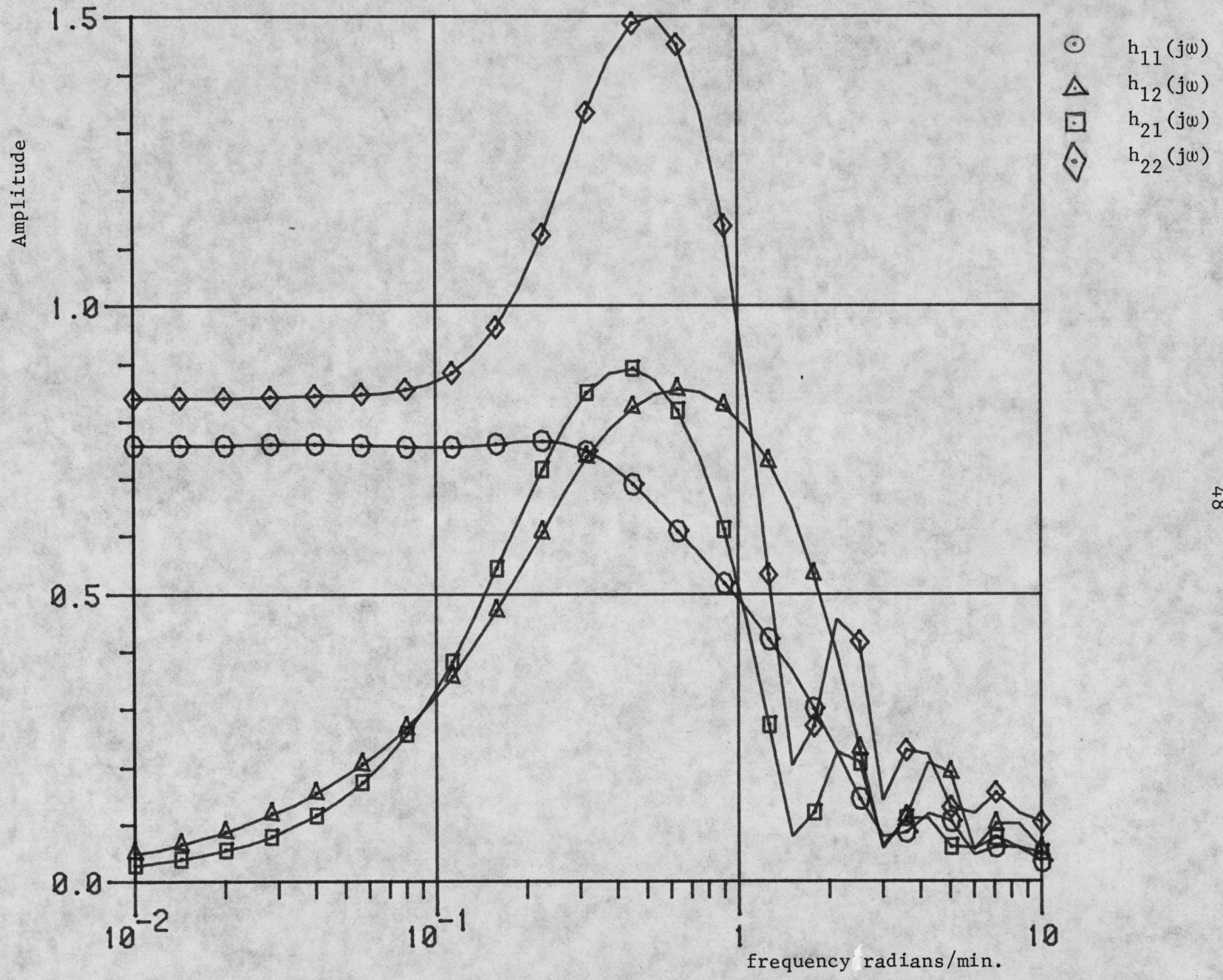

Fig. 6.20. Closed-loop frequency response of system with $M_1(s)$.

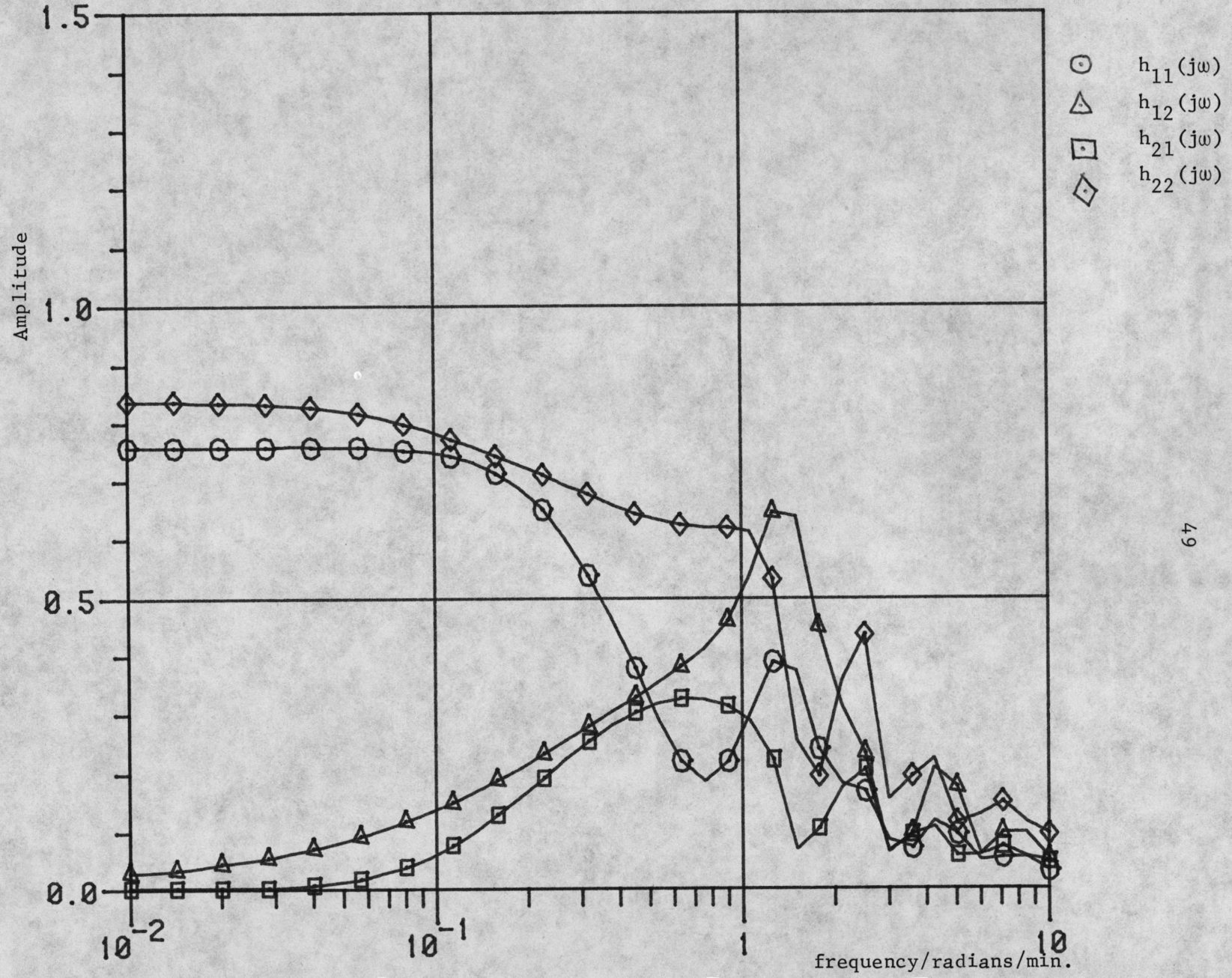

Fig. 6.21. Closed-loop frequency response of system with $M_3(s)$.

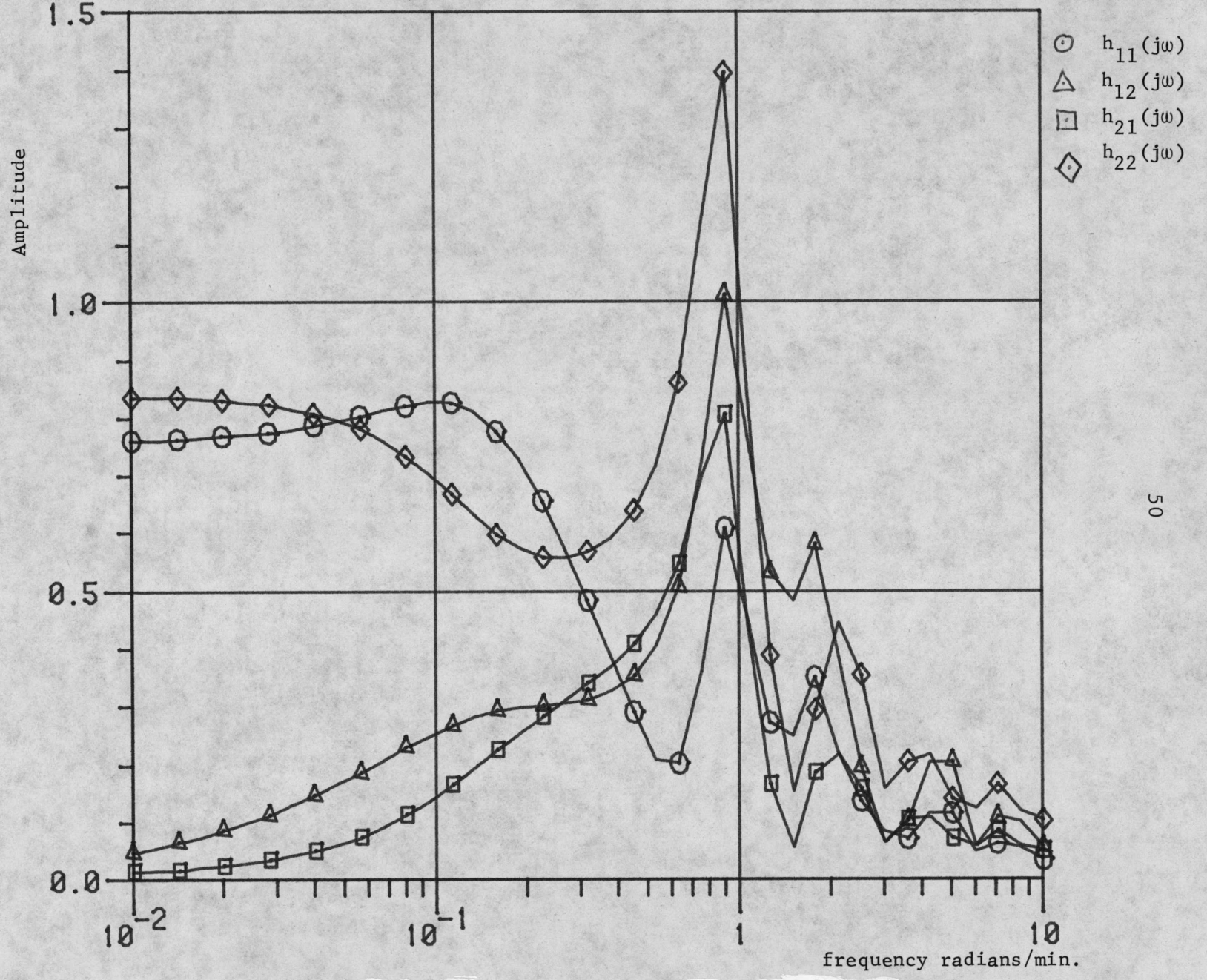

Fig. 6.22. Closed-loop frequency response of system with $M_4(s)$.

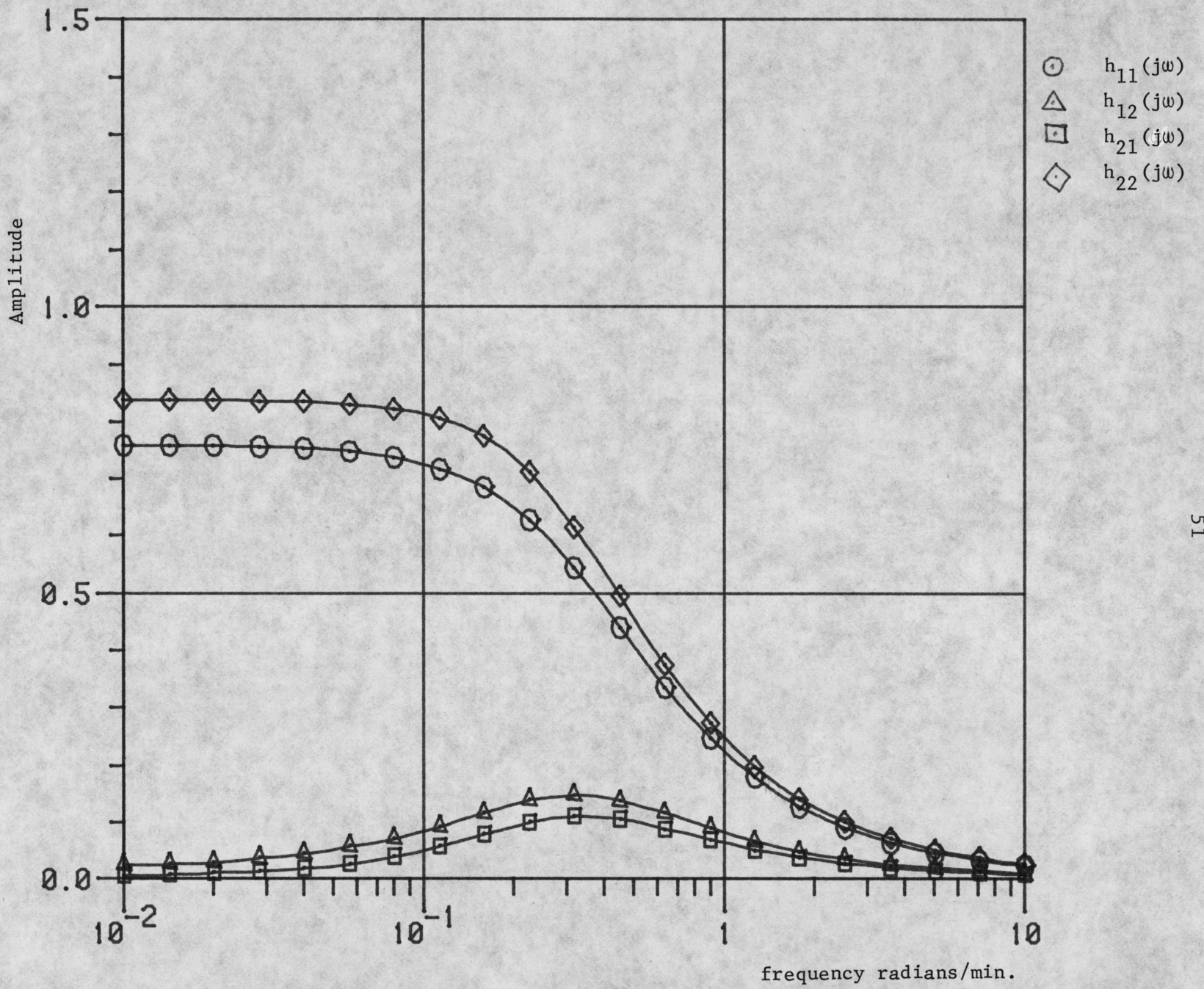

Fig. 6.23. Closed-loop frequency response of system with all delays removed.

A compromise between the model accuracy and delay reduction is obtained with models $M_3(s)$ and $M_4(s)$. Here we observe that the output predictor $M_3(s)$ provides superior performance compared to the input predictor $M_4(s)$. This is a reasonable conclusion in view of the fact that we are feeding back the output signal which is thus more important to preserve than the input relationship.

For the distillation column used in this example, noninteracting control provides better control than predictor control for disturbance inputs. However, for a set-point change, the predictor with $M_3(s)$ shows superior performance in terms of speed and lower IAE values. This observation agrees with the single-variable work of Nielsen [5].

Simulation of the hypothetical system with increased time delays appear to contradict Nielsen's result. The potential benefit of implementing predictor control is increased for plants with greater time delays. However, as before, greater improvement is obtained to a set-point change than to disturbance inputs.

6.6. SYSTEM INTEGRITY TO ACTUATOR OR SENSOR FAILURE

In section 4, we have derived equations relating to failures in any actuator or sensor in a system under predictor control. We now utilize these equations to investigate the robustness of the distillation column under various failure conditions.

The frequency responses of the determinant of the return-difference equation as in (4.12) were plotted for predictor schemes using $M_1(s)$, $M_3(s)$ and $M_4(s)$ and for various values of gain k from 0 to 1.0. The compensator in (6.13) were used throughout, together with proportional gains of 0.5 in both loops. Since the plant is open-loop stable, encirclement of the origin indicates the presence of right half-plane zeros, that is, instability of the system

under the fault condition concerned. It was found that the most severe fault condition occurs when $k = 0$. As k is progressively reduced to zero, the loci move closer to the origin and for some conditions, encircle it.

Table 6.6 summarizes the robustness properties of the various predictor schemes for $k = 0$.

Table 6.6. Robustness to actuator/sensor failure for $k = 0$.

Predictor Type	Actuator 1 failure	Actuator 2 failure	Sensor 1 failure	Sensor 2 failure
with $M_1(s)$	unstable	stable	unstable	unstable
with $M_3(s)$	stable	unstable	stable	stable
with $M_4(s)$	stable	stable	unstable	unstable

It is observed that the different predictor types give rise to widely different robustness properties to actuator and sensor failures. In terms of absolute stability, the predictor with $M_3(s)$ appears to have the best robustness, being unstable only to failure in actuator 2. This is followed by the predictor with $M_4(s)$ and lastly by the predictor with $M_1(s)$. In all cases, even though the system may be stable to a failure, it is close to instability as measured by the closeness to the origin. This is illustrated in Figure 6.24 for the system with $M_3(s)$ for the frequency range from 0 to 1.7 rad./min.

Although no encirclement is seen for any failure condition, a check at high frequencies reveals encirclement for a failure in actuator 2. Further discussion of relative stability in this case can only be made when there is more knowledge of the process concerned and the accuracy of the model.

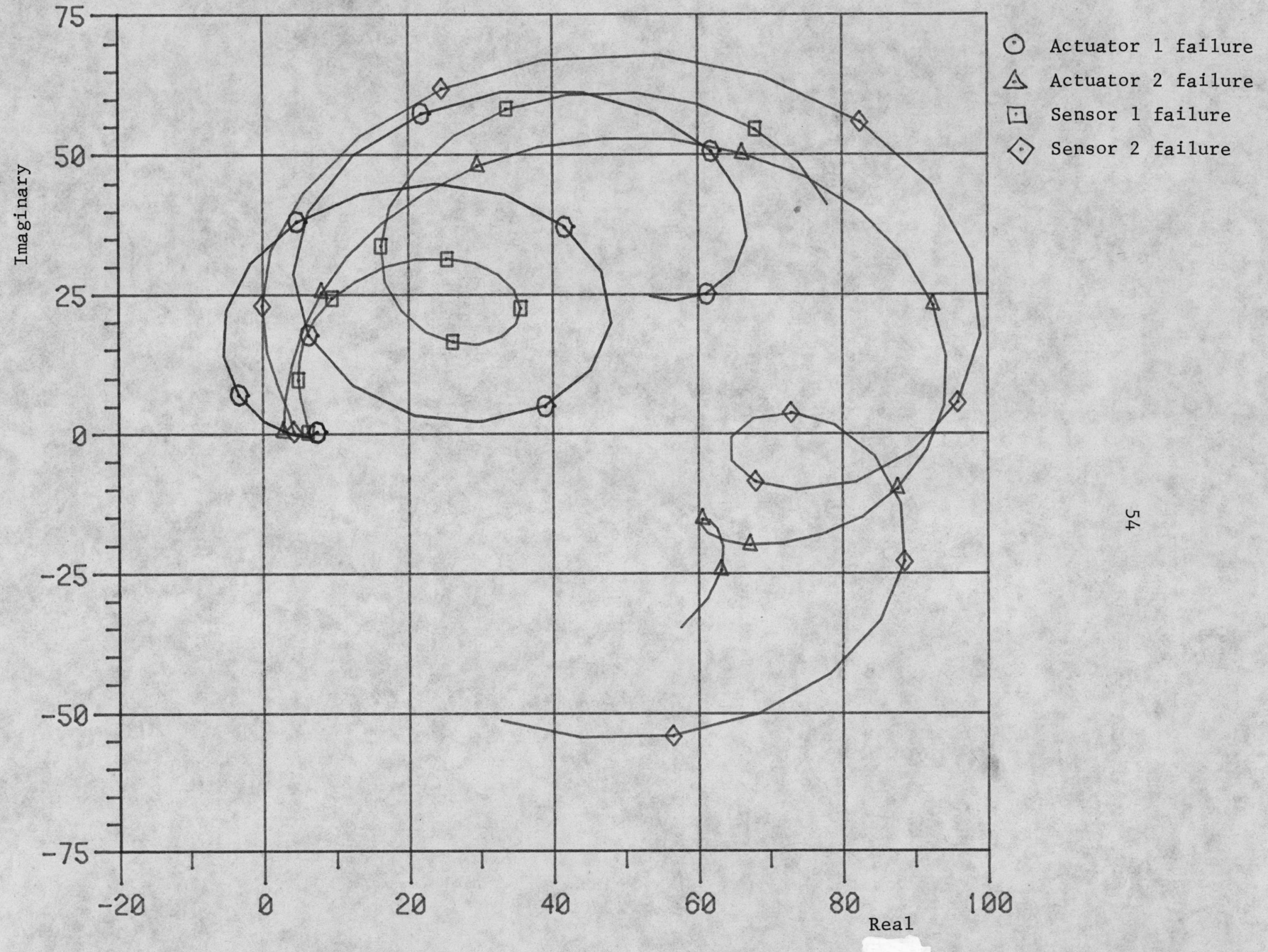

Fig. 6.24. Return-difference plots for actuator or sensor failure.

6.7. PREDICTOR IMPLEMENTATION

In this simulation, we have considered the process as a continuous system. Although simulation of ideal time delay is possible, its implementation in practice is difficult if not impossible. However, in practice a system of this kind would be under computer control. Time delay implementation in this case would be easy and straightforward. Computer control would also allow implementation of predictors of greater complexity than the case considered without any difficulty.

7. CONCLUSIONS

The Smith predictor method has been extended to multivariable plants with arbitrary delays in all control and output variables. A design technique has been proposed and applied to a multivariable distillation column. The simulation results presented lead to the conclusion that the Smith predictor can provide good control even for moderate delays in the plant, and especially to a set-point change. For plants with delays comparable to the plant time constants, the predictor offers greater improvement in performance. Several predictor types have been discussed, which point out the advantages in modifying the conventional predictor.

The question of sensitivity to parameter variation has not been investigated, although some work [8] has previously been carried out. This is an area for further research, as well as the application of this method to other plants, so that more conclusive evidence is obtained.

APPENDIX A: SMITH PREDICTORS FOR MULTIVARIABLE SYSTEMS CONTAINING PURE TIME DELAYS

Consider the multivariable system shown in Figure 2.1, where the state $\underline{x}$ is an n-vector, $\underline{u}$ is an ℓ-vector and $\underline{y}$ is an m-vector; so that matrices G(s), $K_1(s)$ and $K_2(s)$ are of dimensions $m \times \ell$, $\ell \times m$, and $m \times \ell$ respectively.

By breaking the loop at point "a" in the above figure, it can be shown that the return-difference equation is given by

$$F(s) = I_\ell + [I_\ell + K_1(s)K_2(s)]^{-1} K_1(s)G(s) \tag{A.1}$$

Equation (A.1) can be written in the alternative form

$$F(s) = [I_\ell + K_1(s)K_2(s)]^{-1} [I_\ell + K_1(s)K_2(s) + K_1(s)G(s)] \tag{A.2}$$

It is known that the determinant of F(s) gives the following relationship:

$$|F(s)| = \frac{\text{closed-loop characteristic polynomial}}{\text{open-loop characteristic polynomial}} \tag{A.3}$$

Taking the determinant of (A.2), we have

$$|F(s)| = |I_\ell + K_1(s)K_2(s)|^{-1} |I_\ell + K_1(s)K_2(s) + K_1(s)G(s)| \tag{A.4}$$

Note that the first expression on the right-hand side of (A.4) is the determinant of the return-difference of the precompensator, so that its denominator gives the open-loop poles of $K_1(s)$ and $K_2(s)$. However, these open-loop poles also occur in the denominator of the second determinant on the right-hand side of (A.4). Due to the inverse sign, these terms cancel out and we conclude that the closed-loop characteristic equation is simply given

by

$$\left| I_{\ell} + K_1(s)K_2 + K_1(s)G(s) \right| = 0 \tag{A.5}$$

Consider a plant whose transfer function matrix is

$$G(s) = \begin{bmatrix} g_{11}(s)e^{-sT_{11}} & g_{12}(s)e^{-sT_{12}} & \cdots & g_{1\ell}(s)e^{-sT_{1\ell}} \\ g_{21}(s)e^{-sT_{21}} & & & \\ \vdots & & & \vdots \\ g_{m1}(s)e^{-sT_{m1}} & & \cdots & g_{m\ell}(s)e^{-sT_{m\ell}} \end{bmatrix} \tag{A.6}$$

Here $g_{11}(s)$, $g_{12}(s),\ldots,g_{m\ell}(s)$ are purely rational polynomials and the time delays T_{11}, $T_{12},\ldots,T_{m\ell}$ are the result of arbitrary delays present in the plant control and output variables.

In the single-variable case, the Smith predictor eliminates time delays from the closed-loop characteristic equation, so that the characteristic equation depends only on the delayless part of the open-loop transfer function. By analogy, if we observe (A.5) and (A.6), we deduce that the Smith predictor $K_2(s)$ for the multivariable case is given by

$$K_2(s) = \begin{bmatrix} g_{11}(s)(1-e^{-sT_{11}}) & g_{12}(s)(1-e^{-sT_{12}}) & \cdots & g_{1\ell}(s)(1-e^{-sT_{1\ell}}) \\ g_{21}(s)(1-e^{-sT_{21}}) & & & \\ \vdots & & & \vdots \\ g_{m1}(s)(1-e^{-sT_{m1}}) & & \cdots & g_{m\ell}(s)(1-e^{-sT_{m\ell}}) \end{bmatrix} \tag{A.7}$$

It is easy to verify that by substituting (A.7) into (A.5), the closed-loop characteristic polynomial does not involve any time delay terms as they cancel out.

If we have a plant described by the state-space equations

$$\dot{\underline{x}}(t) = A\underline{x}(t) + \sum_{j=1}^{\ell} B_j \underline{u}(t - T_{ij}) \tag{A.8}$$

$$\underline{y}(t) = \sum_{k=1}^{n} C_k \underline{x}(t - T_{0k}) \tag{A.9}$$

where A, B_j, C_k are constant matrices of dimensions $n \times n$, $n \times \ell$, $m \times n$, respectively and $T_{i1},\ldots,T_{i\ell}$ are time delays present in the control variables and $T_{01},\ldots,T_{0n}$ are time delays present in the state variables; then the Smith predictor obtained is as follows:

$$K_2(s) = \sum_{j=1}^{\ell} \sum_{k=1}^{n} C_k G^*(s) B_j (1 - e^{-s(T_{i\ell} + T_{0k})}) \tag{A.10}$$

where

$$G^*(s) = (sI_n - A)^{-1} \tag{A.11}$$

The above derivations can also be obtained by using the manipulated block diagram shown in Figure 2.2 and observing that if D(s) cancels out the effect of G(s), then M(s) alone determines the closed-loop characteristic polynomial. In the conventional predictor M(s) would be the delayless part of the plant transfer function matrix.

Analogous predictors for sampled-data systems can be derived in a similar manner using the methods described above.

REFERENCES

1. SMITH, O. J. M., "Closer control of loops with dead time", Chem. Eng. Prog., 1957, 53, (5), pp. 217-219.

2. SMITH, O. J. M., "A controller to overcome dead time", ISAJ., 1959, 6, (2), pp. 28-33.

3. DAHLIN, E. B., "Designing and tuning digital controllers," Instr. Cont. Syst., 1968, 41, (6), pp. 77-83 and (7), pp. 87-91.

4. MOORE, C.F., et al, "Improved algorithm for direct digital control", Instr. Cont. Syst., 1970, 43, (1), pp. 70-74.

5. NIELSEN, G., "Control of Systems with time delay", Proc. 4th IFAC Congress, Warsaw, 1969.

6. MEYER, C., et al, "An experimental application of time delay compensation techniques to distillation column control", Proc. IFAC Symp. Digital Computer Applic. to Process Control, 1977.

7. ALEVISAKIS, G. and SEBORG, D. E., "An extension of the Smith predictor method to multivariable linear systems containing time delays", Int. J. Control, 1973, 17, (3), pp. 541-551.

8. ALEVISAKIS, G., "Application of the Smith predictor to multivariable systems with time delays", M. Sc. Thesis, University of Alberta, 1972.

9. ROSENBROCK, H. H., "Computer-aided control system design", Academic Press, London, 1974.

10. WOOD, R. K. and BERRY, M. W., "Terminal composition control of a binary distillation column", Chem. Eng. Sci., 1973, 28, (9), pp. 1707-1717.

11. WOOD, R. K. and PACEY, W. C., "Experimental evaluation of feedback, feedforward and combined feedforward-feedback binary distillation column control", Can. J. Chem. Eng., 1972, 50, (6), pp. 376-384.

12. BERRY, M. W., "Terminal composition control of a binary distillation column", M. Sc. Thesis, University of Alberta, 1972.

13. ZALKIND, C. S., "Practical approach to noninteracting control, Pt. 1", Instr. Cont. Syst., 1967, 40, (3), pp. 89-93.

14. ZALKIND, C. S., "Practical approach to noninteracting control, Pt. 2", Inst. Cont. Syst., 1967, 40, (4), pp. 111-116.